



# Finding and Using the World's Gas Hydrates

# 3

Jürgen Mienert, Anne M. Tréhu, Christian Berndt,  
Angelo Camerlenghi, Char-Shine Liu, and Matteo Massironi

## Abstract

For the past 50 years, gas hydrates have been regarded by scientists as part of the hydrocarbon reserves, particularly at governmental institutions. A better understanding of the processes controlling the distribution and dynamics of gas hydrates in nature, especially their sensitivity to changes in gas composition, pressure and temperature, requires both theoretical knowledge of their stability and dynamic behavior and knowledge of how gas hydrates form and where they occur in the sediment. Geophysical data, geochemical data and thermodynamic models indicate that both the rate of response and the total integrated response to climate change in the ocean depend on the location and forms in which hydrates are distributed. Thus, mapping gas hydrates by indirect geophysical methods or through dedicated drilling campaigns is fundamental to all research involving gas hydrates. This includes studies of their role in climate

change, their consequences for slope stability, their role at the base of the food web for benthic ecosystems and their potential as a future energy resource. Here we provide a brief introduction to the occurrence of gas hydrates on Earth, and how this information may assist in detecting them on other planetary bodies.

## 3.1 Introduction—The Location of Gas Hydrates Beneath the Seabed

Active and passive continental margins underlie approximately one third of the world's oceans. Subsurface temperatures in these areas are cold enough and pore pressure is high enough for gas hydrates to form (Fig. 3.1). Gas hydrates are crystalline compounds occurring in the pore space of sediment, creating an ice-like lattice of water molecules surrounding gas molecules (Sloan and Koh 2008). In addition to the requirements for low temperature and high pressure, the stability of gas hydrates also depends on gas and pore water composition, grain size and available pore space. Together, these conditions control the thickness of the gas hydrate stability zone (GHSZ) (Figs. 3.2 and 3.3) (e.g., Riedel et al. 2010), and whether the hydrates will be distributed as small grains in the pore space, as vein-filling sheets, massive layers or as nodules (e.g., Torres et al. 2008). Whether gas hydrates are actually present in the GHSZ depends on the availability of enough free gas and water. It may seem counter-intuitive to expect dry sediment below the ocean floor, but hydrate formation can efficiently consume pore water until there are dry zones within the sediment under very rapid gas flux, allowing gas to escape into the ocean (e.g., Tréhu et al. 2004a). Though most gas trapped in hydrates is methane (e.g., Kvenvolden 1988, Ginsburg and Soloviev 1998), both higher hydrocarbons and CO<sub>2</sub> have also been found in natural gas hydrates (Kvenvolden et al. 1984; Rehder et al. 2008).

J. Mienert (✉)

Department of Geosciences, CAGE - Centre for Arctic Gas Hydrate, Environment and Climate, UiT – The Arctic University of Norway, Tromsø, Norway  
e-mail: [jurgen.mienert@uit.no](mailto:jurgen.mienert@uit.no)

A. M. Tréhu

College of Earth, Ocean, and Atmospheric Sciences, Oregon State University, Corvallis, Oregon, USA

C. Berndt

GEOMAR Helmholtz Centre for Ocean Research Kiel, Kiel, Germany

A. Camerlenghi

Istituto Nazionale di Oceanografia e di Geofisica Sperimentale, Sgonico, Trieste, Italy

C.-S. Liu

Ocean Center, National Taiwan University, Taipei, Taiwan

M. Massironi

Department of Geosciences, University of Padova, Padova, Italy

7INAF, Osservatorio Astronomico di Padova, Padova, Italy

© Springer Nature Switzerland AG 2022

J. Mienert et al. (eds.), *World Atlas of Submarine Gas Hydrates in Continental Margins*,  
[https://doi.org/10.1007/978-3-030-81186-0\\_3](https://doi.org/10.1007/978-3-030-81186-0_3)

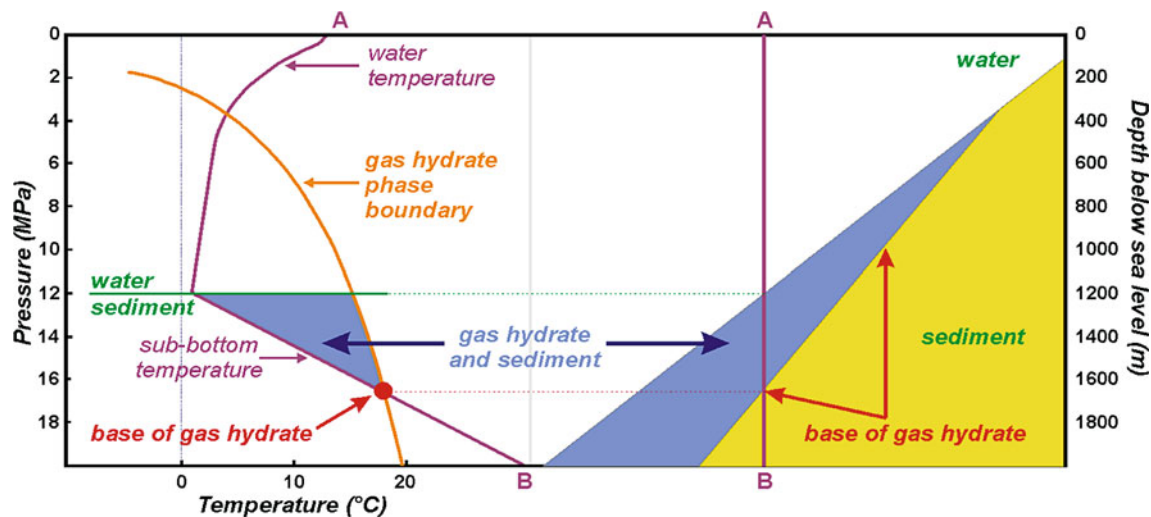


**Fig. 3.1** Example of gas hydrate stability within a continental margin (after Kayen and Lee 1991). Left: methane hydrate stability curve (after Kayen and Lee 1991). Left: methane hydrate stability curve (orange) and temperature-depth profile (purple). Blue regions show GHSZ below the seafloor. Hydrates are also stable in part of the water column, but as they are lighter than water, they will float up and

dissociate. Right: schematic diagram of a continental margin with the location of the phase diagram indicated by the vertical line A–B. GHSZ thickness increases with increasing water depth, and hydrates are unstable towards shallow waters

Gas hydrates are generally found in the uppermost several hundred of meters below the seafloor in continental margins (e.g., Torres et al. 2004, Tréhu et al. 2006, Ruppel and Kessler 2017), and are also commonly associated with permafrost regions (e.g., Dallimore et al. 1999; Collett et al. 2011). At water depths of <400–600 m throughout most of the ocean (depending on the regional oceanic temperature profile), the temperature at the seafloor is too high to permit the formation of gas hydrates (e.g., Fig. 3.1) (Sloan and Koh 2008). Although the GHSZ is theoretically thickest below the deepest parts of the ocean, there is not enough organic matter for biogenic gas production and hence free gas for hydrates to form within the sediment of the deep ocean abyssal plains. Geophysical exploration along continental margins has documented that the focused ascent of warm fluids can locally elevate the subsurface temperature, causing the GHSZ to become thinner (De Batist et al. 2002; Snyder et al. 2004; Crutchley et al. 2014).

### 3.2 History of Gas Hydrate Exploration and Global Assessments of Distribution

The geophysical exploration of continental margins in the 1970s revealed a surprising observation: a seismic reflector that cross-cut other reflectors, which was not the result of

either sedimentary deposition or structural deformation. Because this widespread and enigmatic reflection locally mimicked the seafloor, it was termed the ‘bottom simulating reflector’ (BSR). When the polarity of this reflection is negative, thus indicating a decrease in the seismic velocity of the sediment below the reflection, it is interpreted to represent the base of the GHSZ (BGHSZ). A negative polarity results from the acoustic impedance contrast between hydrate-bearing sediment above and free gas-bearing sediment below (e.g., Stoll et al. 1971; Tucholke et al. 1977; Shipley and Houston 1979). This reflection is thus caused not by lithology or structure, but by a change in the nature of the pore-filling substance.

Sediment coring by the Deep Sea Drilling Project (DSDP Leg 11; DSDP Leg 76) recovered gas hydrates in sediment cores for the first time (e.g., Kvenvolden and McDonald 1985) on the southeast US passive continental margin along Blake Ridge in 1970 (e.g., Paull et al. 1996) and later at the accretionary complex of the Middle America trench (DSDP Legs 66, 67 and 84) (Fig. 3.4). This proved the existence of natural gas hydrates in very different sedimentary environments, supporting the inference from BSR observations that gas hydrates are indeed very common on continental margins. There remains a considerable amount of uncertainty, however, regarding the total amount of gas trapped in hydrates worldwide (e.g., Piñero et al. 2013).

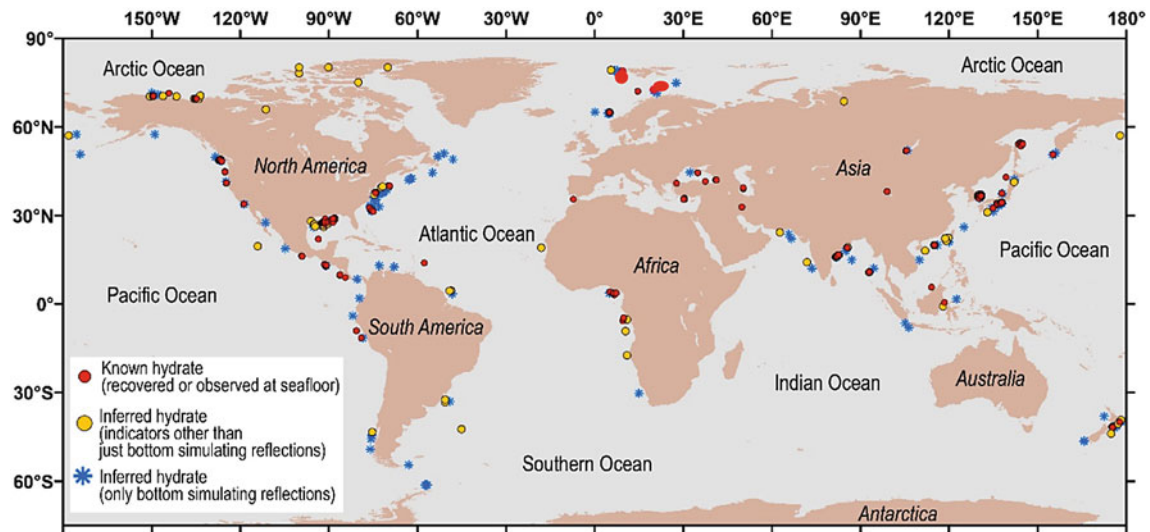


**Fig. 3.2** Top: World map of documented and inferred gas hydrate locations based on the existence of gas hydrate-related bottom simulating reflectors (BSRs) and/or samples from coring operations (modified from Waite et al. 2020, USGS Gas Hydrate Data Base Map).

Bottom: Core sample showing gas hydrate from the Barents Sea offshore northern Norway (credit: hydrate-01\_CAGE20-3, Claudio Argentino, UiT The Arctic University of Norway)

Drilling in the permafrost regions of western Siberia in Russia showed the potential of gas hydrates as an energy resource in the Arctic for the first time. The Messoyakha gas field is in the GHSZ; some of the gas produced in this field may be a result of hydrate dissociation, due to the production-related decrease in gas pressure (e.g., Makogen and Omelchenko

2013). Drilling at Messoyakha likely represents the first time that gas has been produced from permafrost-associated gas hydrates. Shortly thereafter, the Canadian and US American Arctic permafrost region became a focus for international gas hydrate drilling and production tests from gas hydrates (e.g., Dallimore et al. 1999; Collett et al. 2009, 2012).

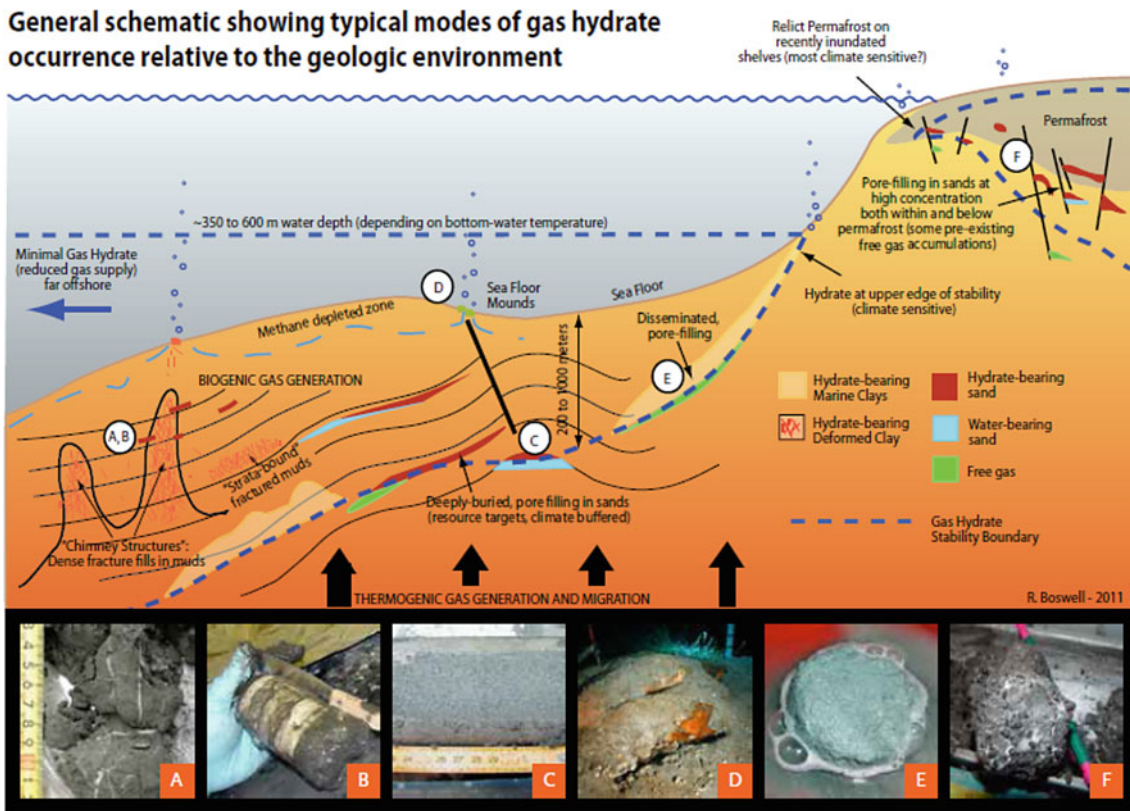


**Fig. 3.3** A–F gas hydrate samples retrieved from different geological environments of continental margins (from Beaudoin et al. (2014a, b); after Boswell and Collett 2011; Boswell et al. 2020)

### 3.3 The Importance of Natural Gas Hydrates

#### 3.3.1 The Role of Gas Hydrates in Climate Change

Because gas hydrate stability depends primarily on temperature and pressure, an important concern is how gas hydrates will respond to global warming, and whether positive or negative feedback will dominate globally. For example, rising seafloor temperatures will result in gas hydrate dissociation, whereas rising sea levels in response to melting ice sheets will increase pressure and help to stabilize gas hydrates (e.g., Kvenvolden 1993; Dickens et al. 1997; Kennett et al. 2003; Ruppel and Kessler 2017). The change in temperature at depth beneath the seafloor lags at the seafloor, whereas the change in pressure is instantaneously transmitted to greater depth. The rate of response and the total integrated response, therefore, depend on the location of hydrates beneath the seabed and how they are distributed (e.g., Archer et al. 2009). The release of methane from hydrate dissociation in ocean environments is likely to: (a) increase the migration dynamics of fluids through

sediment formation in thousands of seeps in the seabed, (b) increase microbial reactions in the ocean, and (c) increase the oxidation of  $\text{CH}_4$  in the ocean, thereby influencing ocean chemistry. The ability to quantify and track the movement of global seafloor methane emissions from gas hydrate dissociation remains highly uncertain, while the role of microbes in controlling the flux of methane from the seafloor to the ocean also remains poorly understood. Knowledge of the global distribution of gas hydrates along continental margins, from both deep to shallow geographic settings, is essential for evaluating the potential impact of climate change on various environments (e.g., Kennett et al. 2000; Higgins and Schrag 2006; Dickens 2011; Ruppel and Kessler 2017). This world atlas offers a unique compilation of geophysical data, providing insight into the areas of gas hydrate formation in the oceans of the world. Because climate change is the primary driver of environmental change and has an impact on various ocean–atmosphere interactions, this world atlas provides a valuable resource for those who aim to understand the response of hydrate systems in different physiographic and geographic settings, from high to low latitudes and from past, present and anticipated future conditions.



**Fig. 3.4** Deep Sea drilling Project (DSDP) vessel Glomar Challenger. The upper right shows Keith Kvenvolden, who studied the submarine gas hydrates in the middle American Trench off Guatemala and Costa Rica, participating in Leg 84 (from photo archive Scripps Institution of Oceanography UC San Diego Library)

### 3.3.2 Hydrates as a Control on Benthic Ecosystems

Biogenic methane production depends on the rate that methanogenic archaea convert organic carbon to methane, which is a function of ambient temperature and other environmental boundary conditions (e.g., Boetius et al. 2000). Because temperature increases with depth beneath the seafloor, there is a maximum depth at which archaea are still active and produce methane from organic matter (e.g., Parkes et al. 1994). Water flux through a given sedimentary environment is also a driver for methanogenic productivity (e.g., Knittel and Boetius 2009); as permeability and water flux decrease, so does productivity of methane.

There is a zone close to the seabed that is undersaturated in methane due to the microbial reduction of sulfate, which oxidizes methane and produces sulfide (Borowski et al. 1999; Boetius and Wenzhöfer 2013) (Fig. 3.5). The thickness of this zone depends on the rates of (largely buoyancy-controlled) upward methane migration and diffusion-controlled downward sulfate migration. The base of this zone is referred to as either the sulfate methane interface (SMI) or the sulfate-methane transition zone (SMTZ). This process prevents the formation of gas hydrates

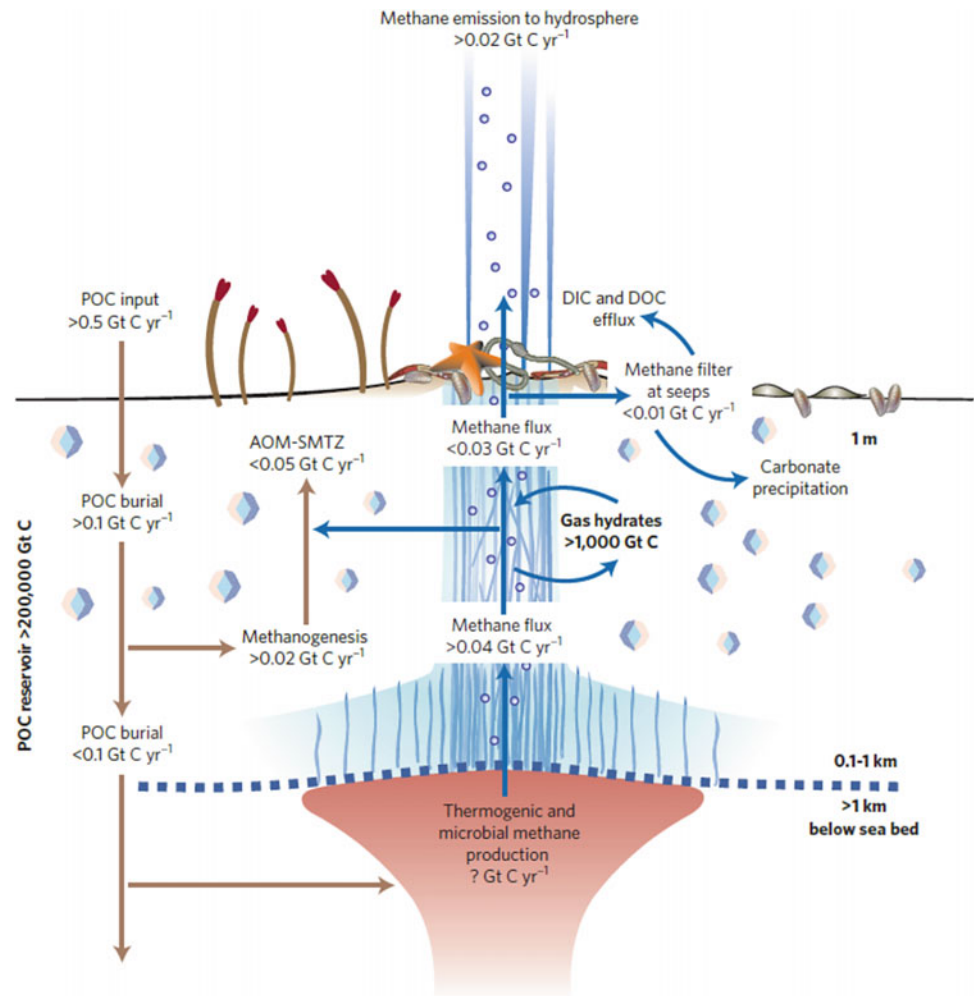
at or near the seabed, except in areas with very high rates of methane advection (Borowski et al. 1999). The resulting high concentrations of hydrogen sulfide support chemosynthetic biological communities that gain energy from sulfide oxidation. These communities are diagnostic of the presence of gas hydrates in the shallow subsurface and can include the filamentous sulfur bacteria *Beggiatoa*, the clam *Calyptogena* or the bivalve *Acharax* (Treude et al. 2003). The Gulf of Mexico (e.g., MacDonald et al. 2005) (Fig. 3.6) and the Cascadia Margin (e.g., Scherwath et al. 2019; Thomsen et al. 2012) are two notable examples of regions where the dynamics of thermogenic and/or biogenic gas hydrates have been monitored in relation to chemosynthetic biological communities (Boetius and Wenzhöfer 2013; Sahling et al. 2016). Thermogenic gas is known to migrate upward into the GHSZ in these areas.

### 3.3.3 The Role of Gas Hydrates in Slope Stability

Gas hydrates occur in various forms in the sediment, ranging from finely distributed or fracture-filling veins to massive meter-scale accumulations (Holland et al. 2008). These morphologies largely depend on sediment type, fault systems and gas source. As hydrates may cement sediment and increase the shear strength, their dissociation may reduce the shear strength when it is accompanied by a pore pressure increase due to gas release, although the latter process is self-limiting. Theoretically, gas hydrate dissociation may be an efficient process for destabilizing the seafloor (e.g., Kayen and Lee 1991; Sultan et al. 2004) (Fig. 3.1), which relates to the clathrate gun hypothesis. This hypothesis proposes that initial ocean warming may lead to an increased occurrence of slope failure and methane release that, in turn, may lead to further warming and more landslides (e.g., Kennett et al. 2000; Maslin et al. 2010). The Storegga Slide was cited early on as a potential candidate for this process (Mienert et al. 2002). However, despite two decades of research at continental margins on the proposed link between hydrates and slope stability (e.g., Henriot and Mienert 1998), no conclusive evidence has been produced that hydrate dissociation has caused a major submarine landslide (Mienert et al. 2005). It must be noted, however, that submarine landslides remove most of the geological evidence for their triggering mechanisms, making conclusive determinations unlikely. A study from the joint industry/academia Ormen Lange project (Bryn et al. 2005) at the 8200 year old Storegga Slide scar (Haflidason et al. 2005) provided geophysical, geological and geotechnical evidence suggesting that failure planes relate to the strain softening behavior of marine clays in response to rapid sediment loading in glacial times. This

**Fig. 3.5** Model shows interactive processes of cold seep methane and carbon fluxes at continental slopes (from Boetius and Wenzhöfer 2013).

POC = Particulate Organic Carbon; AOM = Anaerobic Oxidation of Methane; SMTZ = Sulfate-Methane Transition Zone, DIC = Dissolved Inorganic Carbon; DOC = Dissolved Organic Carbon



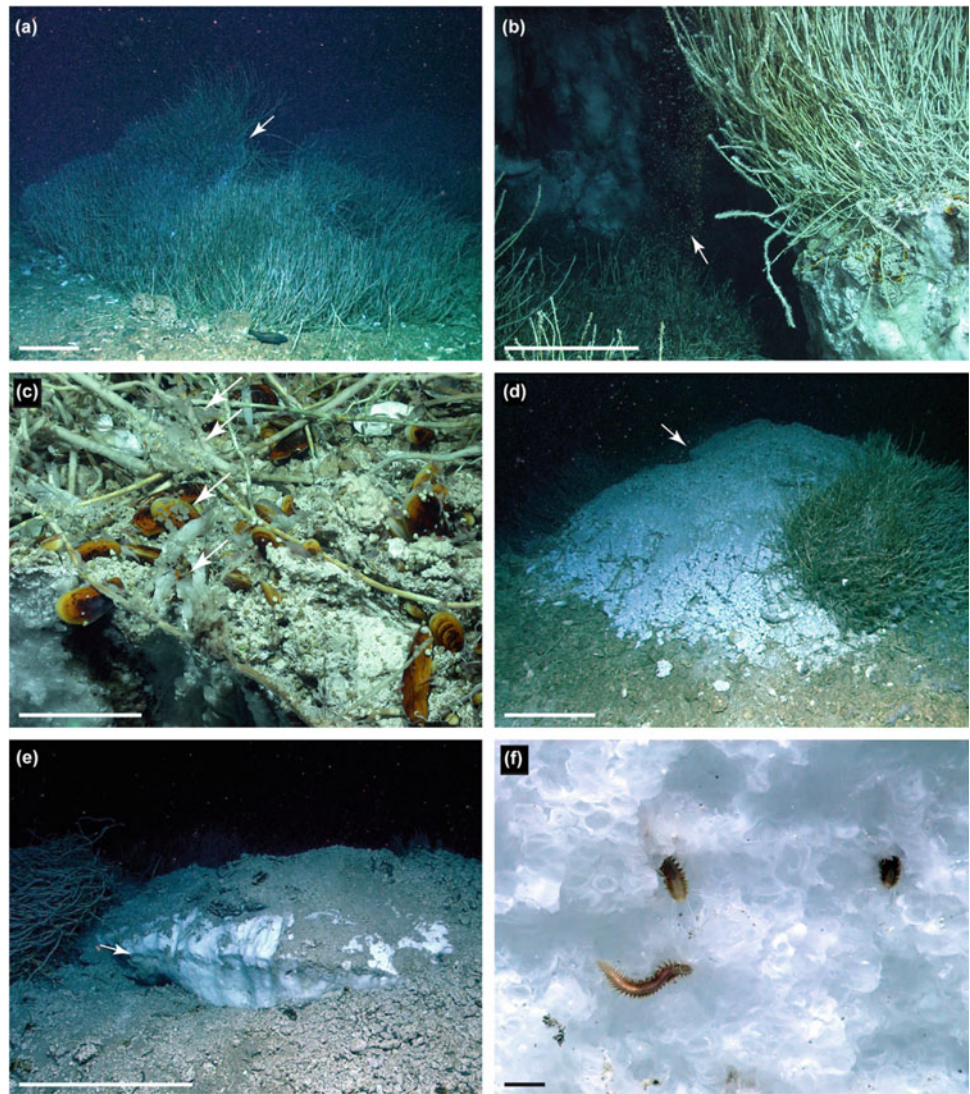
generated excess pore pressure and supported the reduction of the effective shear strength in the underlying clays, leading to the retrogressive formation dynamics of the giant slope failure during the deglaciation period. Ultimately, it is thought that the slide was most likely triggered by a large earthquake (Bryn et al. 2005). Large scars have been left on the continental slopes of the world, mainly from retrogressive submarine slope failures, making it difficult to attribute a specific event to a particular failure mechanism due to the concurrent weakening of the slopes (e.g., Paull et al. 2021). Though hydrate dissociation is likely not a trigger (just as rapid sediment loading is not a trigger) for slope failure, it should be conducive in reducing shear strength during hydrate dissociation, allowing smaller magnitude earthquakes to trigger slope failure. Quantifying this effect compared to other possible hypotheses has been the real challenge. Hydrate dissociation, degassing and excess pore pressure evolution are topics that new studies may wish to investigate on upper continental slopes (e.g., Leynaud et al. 2007; Sultan et al. 2004).

### 3.3.4 Hydrates as a Future Energy Source

The very high initial estimate of gas hydrate volume was more than 10,000 Gt of carbon (Kvenvolden 1988), which was revised downward to 500 Gt (Milkov and Etiope 2005) before being revised again to settle at estimates between 1500 and 4500 Gt (Piñero et al. 2013; Kretschmer et al. 2015; Archer and Buffet 2005). Although there is still a high level of uncertainty regarding the total number of hydrates, they represent a considerable fossil fuel resource. For this reason, several countries have invested in hydrate research programs to assess the potential use of gas hydrates as a future energy resource (Fig. 3.7).

The physical and chemical properties of gas hydrates are already quite well understood from a theoretical and laboratory perspective (Sloan 1998), and their formation and recognition criteria have seen continuous developments over the past decades (e.g., Shipley and Houston 1979; Ginsburg and Soloviev 1998; Bünz et al. 2005; Westbrook et al. 2008). Nevertheless, certain technical challenges must be

**Fig. 3.6** Seafloor images from the Gulf of Mexico's Tsanyao Yang Knoll (MARUM ROV QUEST Dive 361) (from Sahling et al. 2016). The images with a scale bar of 50 cm show **a** Vestimentiferan tube worm bushes, **b** rising gas bubbles (arrow) and formation of hydrates at adjacent walls, **c** surface closeup from the same location with rising bubbles. Gas hydrates form below a layer of authigenic carbonates featuring mytilids, vestimentifera, gastropods and shrimps on top (Note: scale bar 10 cm), **d** gas hydrate mound (arrow) with closeups in **e** and **f**. (Note: scale bar for **f** is 1 cm with closeup of a porous hydrate inhabited by ice worms/cf. *Hesiocaeca methanicola*) (All images courtesy of MARUM)



addressed before gas hydrate formates can be considered a viable energy source. These include the geomechanical stability of the hydrate reservoirs, the production of sand and water, the unknown changes in reservoir properties due to production and the reformation of hydrates elsewhere in the reservoir due to the endothermic nature of hydrate dissociation processes (e.g., Dallimore et al. 2008; Yamamoto et al. 2014). Whether a particular gas hydrate deposit has potential as an energy resource largely depends on how the hydrate is distributed within the sediment (Boswell and Collett 2011; Johnson 2011).

### 3.3.5 Carbon Capture and Storage (CCS) in Gas Hydrate Reservoirs

Solutions proposed to control global temperature increases and slow climate change must include measures for

stopping the industrial release of  $\text{CO}_2$  into the atmosphere (e.g., Ehlert and Zickfeld 2017; Masson-Delmotte et al. 2018). During the Industrial Age, the concentration of this greenhouse gas increased from  $\sim 280$  ppm in the year 1750 to  $\sim 417$  ppm in March 2021, with a continual rise of  $\sim 2.5$  ppm per year between 2010 and 2020 ([https://www.esrl.noaa.gov/gmd/webdata/ccgg/trends/co2\\_data\\_mlo\\_anngr.pdf](https://www.esrl.noaa.gov/gmd/webdata/ccgg/trends/co2_data_mlo_anngr.pdf)). This poses nearly insurmountable challenges, as entirely avoiding fossil fuels and their subsequent  $\text{CO}_2$  emission is not yet feasible in 2021, or in the near future. Most scenarios proposed by the Intergovernmental Panel on Climate Change (IPCC), therefore, include the geological storage of  $\text{CO}_2$  (e.g., in saline aquifers or depleted hydrocarbon reservoirs). While the storage of  $\text{CO}_2$  in geological formations does pose risks, such as the potential leakage of the gas into the atmosphere, the capture of  $\text{CO}_2$  in gas hydrates may circumvent this problem, as  $\text{CO}_2$  hydrate is a solid with low mobility (Ohgaki et al.

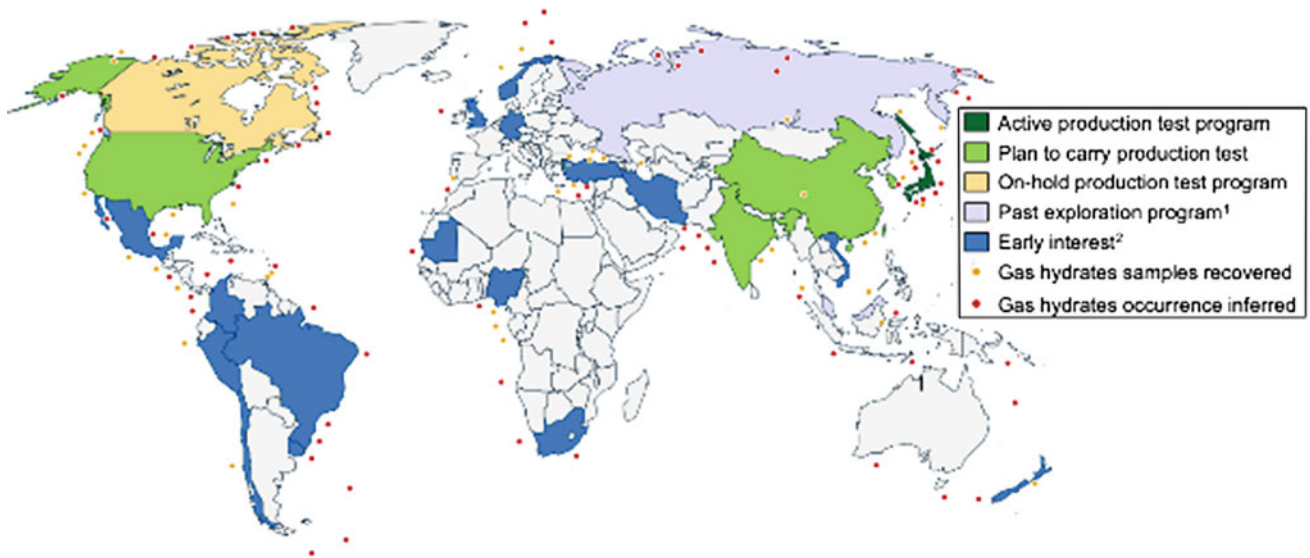
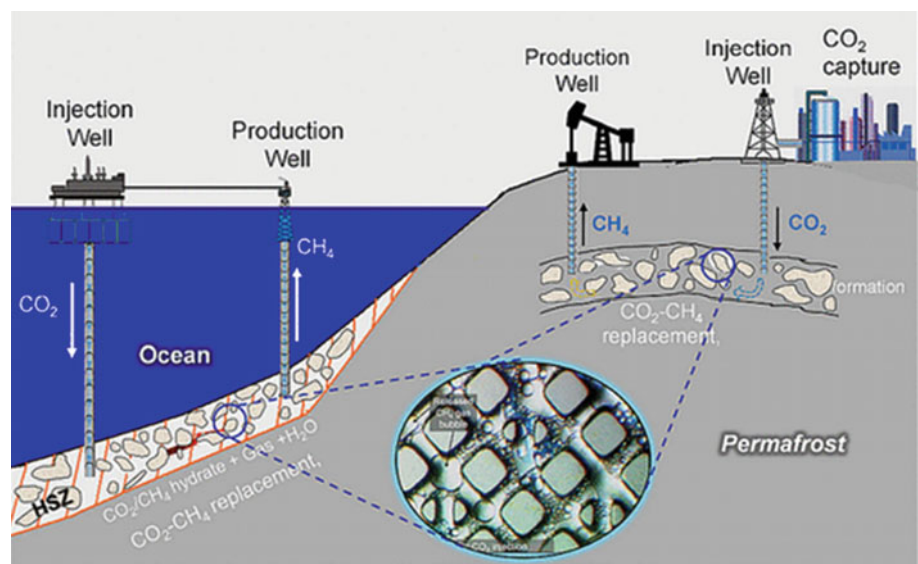


**Fig. 3.7** Countries active in gas hydrate development as a potential energy source (from Decourt et al. 2015; SBC Energy Institute). Note that Fig. 3.2. lacks some sites offshore S Australia and Indonesia, which are indicated here

1996). Since  $\text{CO}_2$ -hydrates are more stable than methane-hydrates, it should be possible to inject  $\text{CO}_2$  into the seabed and capture it as a  $\text{CO}_2$ -hydrate, while simultaneously producing methane from a methane-hydrate. (e.g., Pandey and Sangwai 2020) (Fig. 3.8). While there have been significant research efforts into this concept, it is still unclear whether it is economically viable.

**Fig. 3.8** Schematic diagram of methane production from hydrates in ocean and permafrost; injection and replacement of methane with  $\text{CO}_2$  (from Jadhawar et al. 2021)



## 3.4 Evidence of Submarine Gas Hydrates

### 3.4.1 Geophysical Evidence

Gas hydrates have been identified in permafrost at high latitudes, as well as in active and passive continental margins



at both high and low latitudes. Hydrate-bearing sedimentary sections range in thickness from only a few centimeters to tens of meters, depending on the geological, chemical and physical parameters (You et al. 2019).

Geophysical surveys for gas hydrates along continental margins are commonly achieved through a combination of seismic and electromagnetic methods (see Riedel et al. 2010 and references therein). The identification and subsequent mapping of gas hydrate-related BSRs often represent the earliest evidence in detecting the presence of gas hydrate-bearing sediment beneath the seabed (Kvenvolden 1993). The compressional wave (P-wave) velocity of pure gas hydrates in laboratory measurements reaches 3.3–3.8 km/s (Sloan and Koh 2008), which is high compared to the velocity of unconsolidated sediment. Hydrates in pore space should therefore increase the bulk velocity of the sediment in comparison to sediment without hydrates. The presence of free gas in sediment, however, has an even more distinct effect by decreasing the P-wave velocity. The integration of data from the Deep Sea Drilling Program together with seismic analyses have shown that the occurrence of a BSR is mainly the result of free gas (Paull et al. 1996). Therefore, it is difficult to estimate the number of hydrates present by mapping the BSR alone. Moreover, seismic and drilling data have shown that the absence of a BSR reflects the absence of free gas below the GHSZ, but does not rule out the presence of gas hydrates above it (Paull et al. 1996). Because gas hydrate formation depends on the presence of free gas, however, gas hydrate occurrence without a BSR is probably quite rare; thus, the BSR remain a useful indicator

for the presence or absence of gas hydrates (Fig. 3.9). It should be noted that BSRs can only be unequivocally identified when they cross stratigraphic reflections, and are difficult to identify in areas of horizontally stratified sediment.

A more reliable method for the identification of gas hydrates is, therefore, a detailed seismic velocity analysis. This could be achieved through the full waveform inversion of surface seismic data, for example (Singh et al. 1993; Delescluse et al. 2011). Unusually high P-wave velocity increases above the theoretical BGHSZ (Fig. 3.10a) may reveal the presence of hydrates, even when no BSR is clearly visible (Fig. 3.10b).

Even greater levels of certainty can be achieved using 3-component ocean bottom seismometers, as they not only provide information on the P-wave velocities but also on the S-wave velocities (Bünz et al. 2005). The ways in which hydrates are distributed in the sediment (e.g., in pore space, as grain coating or cementing hydrates) will also affect the S-wave velocity (Chand et al. 2003). A drop in P-wave velocity without a drop in S-wave velocity below the BGHSZ is indicative of free gas. If the S-wave velocity shows a continuous trend beginning high above the BGHSZ, going down through the free gas zone and beyond, deviations of P-wave velocity from a background trend in this interval can be used to constrain hydrate saturation levels.

Perhaps one of the most sophisticated studies to constrain hydrate saturation levels from seismic data used a 4 km long multicomponent ocean bottom cable line (Fig. 3.11) (Andreassen et al. 2003; Bünz and Mienert 2004). The

**Fig. 3.9** Multichannel seismic line offshore mid-Norway, showing a BSR and the location of the ocean bottom cable (OBC) 4C line (from Bünz and Mienert 2004). The bottom simulating reflector (BSR) runs parallel to the seabed at the northern flank of the Storegga Slide. The termination of high amplitude anomalies as indicated by arrows marks the base of the gas hydrate stability zone (BGHSZ). Vertical acoustic pipes pierce through the BSR and reach all the way to the seabed where they connect to pockmarks, indicating fluid flow through the GHSZ (Bünz and Mienert 2004)

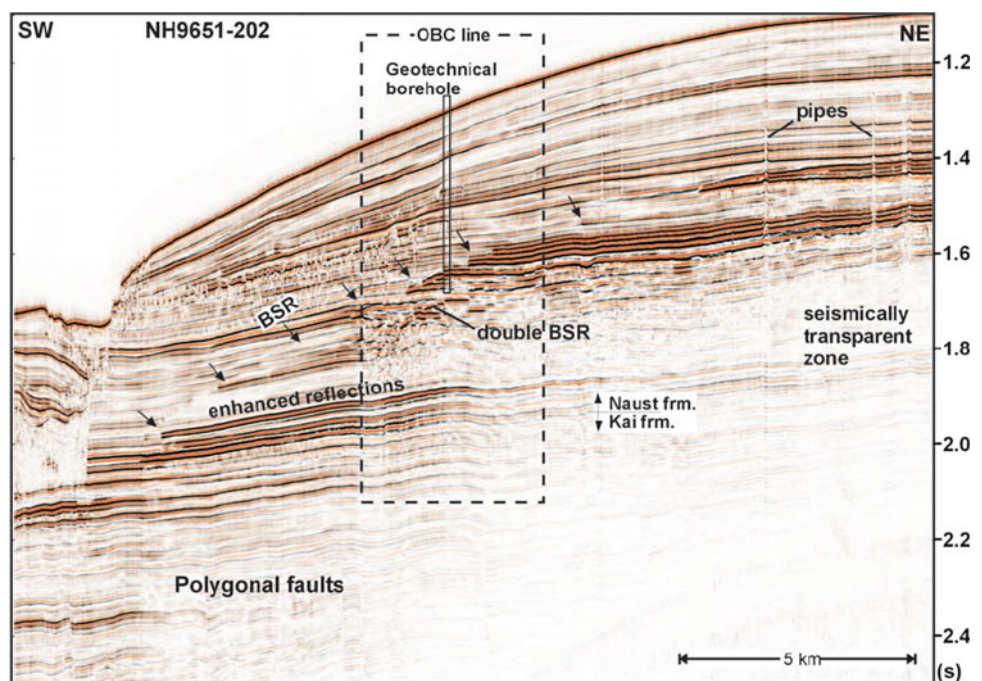


**Fig. 3.10** **a** P-wave seismic velocities from the full waveform inversion of a 9 km long surface towed streamer. LVZ means low velocity zone. **b** Corresponding seismic amplitude plot (after Delescluse et al. 2011)

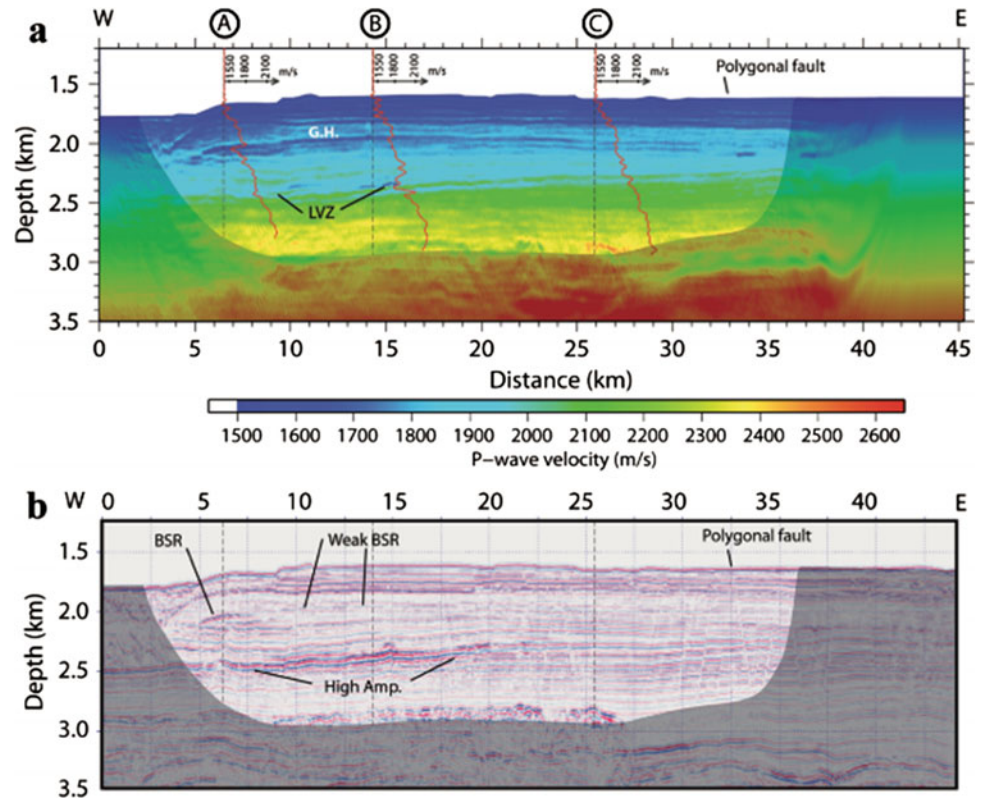
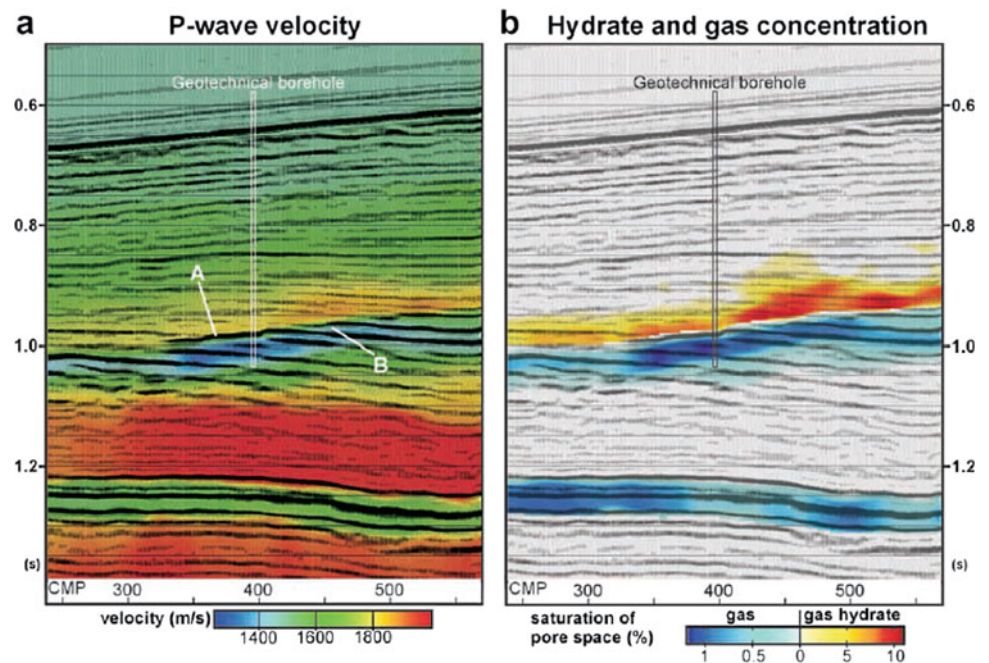


**Fig. 3.11** **a** Seismic section with geotechnical borehole location integrated with color coded P-wave velocities (from Bünz and Mienert 2004). The BSR correlates clearly with a velocity inversion from  $\sim 1800$  to  $1400$  m/s. **b** Seismic section with geotechnical borehole location, overlain with hydrates, and the gas saturation of pore space in sediment calculated using the rock physics model from Helgerud et al. (1999)

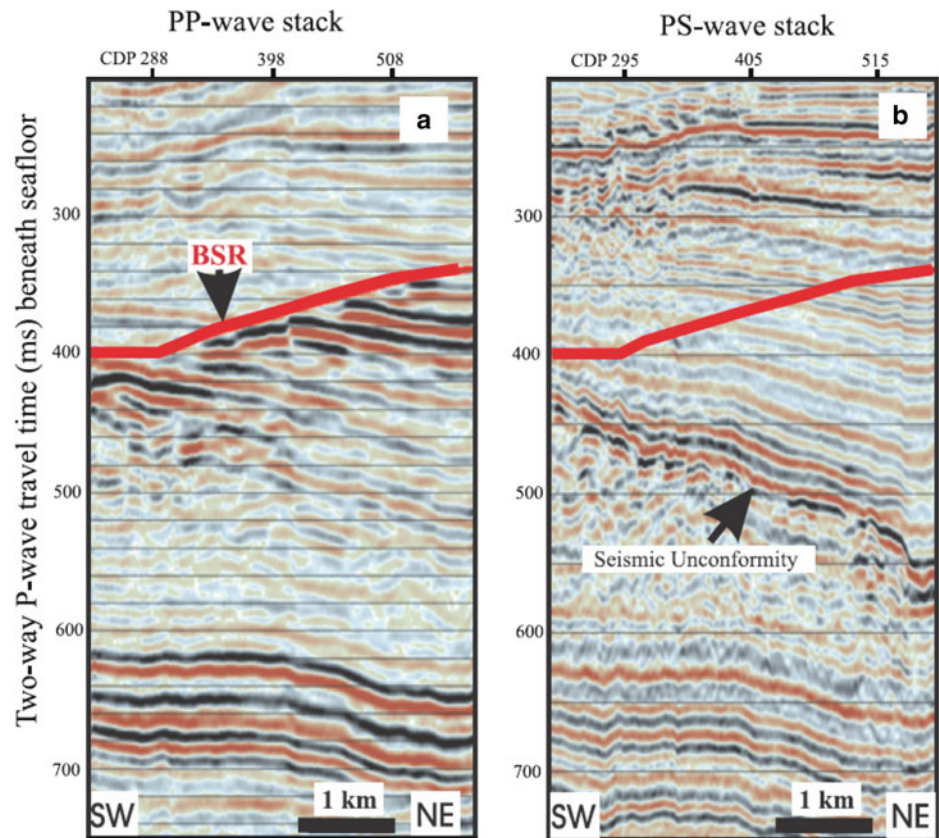


observed BSR corresponds with a drop in P-wave velocity, from  $1700\text{--}1800$  m/s above the BSR to  $<1500$  m/s beneath it. It can be easily identified in the reflection seismic profile (Fig. 3.11), showing all the characteristics of a BSR (i.e.,

subparallel to the seabed, depth consistent with the predicted BGHSZ, phase reversal).

The data collected through the ocean bottom cable (OBC) demonstrates its potential in gas hydrate investigation

**Fig. 3.12** A P-P section of the OBC line shows a clear BSR (marked by a red line) while **B** the P-S does not. The P-S section may indicate a lack of increase in sediment shear strength due to a lack of hydrate cementing. A seismic unconformity is clearly visible in the P-S section (from Andreassen et al. 2003)



through the comparison of the P-P seismic section with the P-S seismic section (Fig. 3.12). While a strong BSR is observed on the P-P section, no BSR exists on the P-S section, indicating that gas hydrate-bearing sediment does not provide enough cementation of the sediment matrix for the shear modulus to increase. While both gas concentration levels beneath the BSR and hydrate concentration levels above it vary, they are still generally low (<2%) (Andreassen et al. 2003).

### 3.4.2 Quantifying Hydrates Through Chemical Measurements of Cores

The DSDP, ODP and IODP recoveries of sediment cores from gas hydrated sediment in continental margins have provided needed insights into the geological controlling factors (i.e., porewater, temperature, gas composition, grain sizes) for the growth and decay of natural gas hydrates (e.g., Ginsburg and Soloviev 1998). Since hydrates begin to decompose as soon as a sediment core leaves its in-situ pressure stability field at sub seabed depth, it is difficult to measure gas hydrate amounts from recovered cores. This obvious problem led to several technological developments, including logging while drilling (LWD) (Saito and Goldberg 1997), the measurement of indirect chemical effects such as

pore water freshening, the scanning of cores with infrared immediately upon retrieval (e.g., Long et al. 2010) and pressure core samplers (PCS) that maintain the sample at in situ pressure (Holland et al. 2008).

The process of hydrate formation affects the pore water geochemistry in two ways (Ussler and Paull 1995): (1) positive chlorinity anomalies exist in hydrate-bearing sediment (e.g., Tomaru et al. 2006), but melting hydrates release fresh water, causes a freshening of the pore water, and (2) water molecules containing heavier oxygen and hydrogen isotopes are preferentially incorporated into the hydrate molecules.

Porewater freshening as a proxy of decomposed gas hydrates in core sediment was first proposed after the drilling of ODP Leg 112 (Kvenvolden and Kastner 1990) and later confirmed in ODP Leg 146 (Westbrook et al. 1994; Kastner et al. 1995). As expected, intervals with low chlorinity levels were also found to contain excess concentrations of head-space methane released by decomposing hydrates. The calculation of original hydrate concentration levels based on pore water freshening typically assumes a chlorinity anomaly identified with respect to a reference value of sea water chlorinity. Egeberg and Dickens (1999) modelled the most likely reference chlorinity profile expected in a sedimentary sequence, taking into account (a) the position of the sulfate-methane transition zone, (b) the molecular diffusion of ions excluded during the process of hydrate formation,

(c) the processes of hydrate dissociation at the base of the stability zone, and (d) the glacial-interglacial bottom water salinity fluctuations.

Negative thermal anomalies in sediment cores, measured directly and immediately with thermometers inserted through the core barrel after recovery, have qualitatively suggested the ongoing melting of hydrates (e.g., Westbrook et al. 1994). This is because the decomposition of hydrates, which also causes the freshening of pore water, is endothermic (Sloan and Koh 2008). The technique has been improved with the use of infrared thermal imaging (ODP Leg 204 and beyond), where the calibration of temperature anomalies in hydrate-bearing, sand-rich layers was established by Weinberger et al. (2005) and Long et al. (2010).

The enrichment of heavy isotopes ( $^{18}\text{O}$  and D) in pore water collected from gas hydrate-bearing sediment has provided information on the abundance of hydrates and their mechanisms of formation in the Oregon margin (Tomaru et al. 2006). Isotopic anomalies must be calculated against a reference curve normally obtained from a gas hydrate free site in the vicinity. Hydrate melting should influence pore water such that it becomes less saline and the oxygen becomes isotopically heavier. The influence of gas hydrate formation and decomposition on the oxygen isotopic composition of interstitial water should be considered in the interpretation of the isotopic composition of benthic foraminifers living in gas hydrate-bearing sediment and in methane-derived authigenic carbonates (Dessandier et al. 2020).

### 3.4.3 Borehole Logging

Wireline downhole logging (DHL) and logging while drilling (LWD) in boreholes to identify permafrost or hydrate-bearing layers are similar in many respects (e.g., Ruppel et al. 2016). These indirect methods allow for the measurement of in-situ conditions of the geophysical and geochemical properties of surrounding formations (Goldberg and Saito 1998). If gas hydrates are present, there may be an increase in electrical resistivity, a decrease in density, a decrease in temperature and an increase in both compressional wave and shear wave velocities relative to the expected background values for these parameters. Marked increases in shear wave velocity with increasing hydrate concentration levels, for example, have been measured in the Mallik well of the Mackenzie Delta in Canada (e.g., Collett et al. 1999).

Downhole logging demonstrated as early as DSDP LEG 84 that sonic, density, resistivity, neutron porosity and gamma ray well log data enabled the identification of hydrate-rich layers (Mathews and von Huene 1985), with

detection reliability decreasing in silty-clayey layers featuring minor amounts of hydrate.

Downhole logs, unlike cores, provide in-situ measurements that assist in identifying both the location and amount of gas hydrates in the subsurface by assessing their natural state. It allows a more accurate assessment of the volumes of gas hydrates and free gas within the host sediment (e.g., Collett 1993; Goldberg et al. 2000, 2010; Helgerud et al. 2000). In general, the two most difficult reservoir parameters to determine on ship-board cores are porosity and the levels of gas hydrate saturation. Downhole log evaluation uses techniques developed by the hydrocarbon industry to quantify these difficult reservoir parameters, including resistivity, density, neutron porosity and sonic logs (e.g., Goldberg et al. 2010). Some applications use a comparison of porosity measurements taken through different techniques for the quantification of gas hydrates (Fig. 3.13).

While wireline logging measurements can be made in more rigid permafrost, continental margin sedimentary environments often comprise unconsolidated sediment in the upper 100 m below sea floor (mbsf), creating an unstable hole that makes logging impossible. Logging While Drilling (LWD) overcomes this limitation, however, allowing researchers to log over the entire section of the gas hydrate stability zone. LWD was first used in offshore gas hydrate research during the initial phase of ODP Leg 204 to provide a ‘road map’ in guiding the subsequent coring strategy (Tréhu et al. 2004b, 2006; Riedel et al. 2010). The advanced application of geophysical logs in boreholes provides one of the few ways to gain insight into the natural (i.e., in-situ) hydrate environment with high (<0.1 m) resolution data, for which this atlas provides several examples.

## 3.5 Gas Hydrates in the Solar System: Applying Lessons from Earth

Is it possible that gas hydrates exist on other planetary bodies such as Mars, the icy moons of Jupiter or comets? Based on the known requirements of Earth, it takes water, gas, low temperature and high pressure for hydrates to form (e.g., Sloan 1998). There is geomorphological evidence that an ocean existed on Mars around  $\sim 4$  Ga (Clifford and Parker 2001), along with channels and lakes such as the Jezero crater, where the rover *Perseverance* landed in 2021 (Fig. 3.14). Carbonates have also been found along the inner rim of the Jezero crater (black circle) (Fig. 3.14), formed more than 3.5 billion years ago (Horgan et al. 2020). On Earth, carbonate rock builders can be either abiogenic (e.g., through the serpentinization of mafic rocks; McDermott et al. 2015) or biogenic (e.g., through the shells of corals and other shellfish, or by microbial life activity; e.g., Zhu and Dittrich

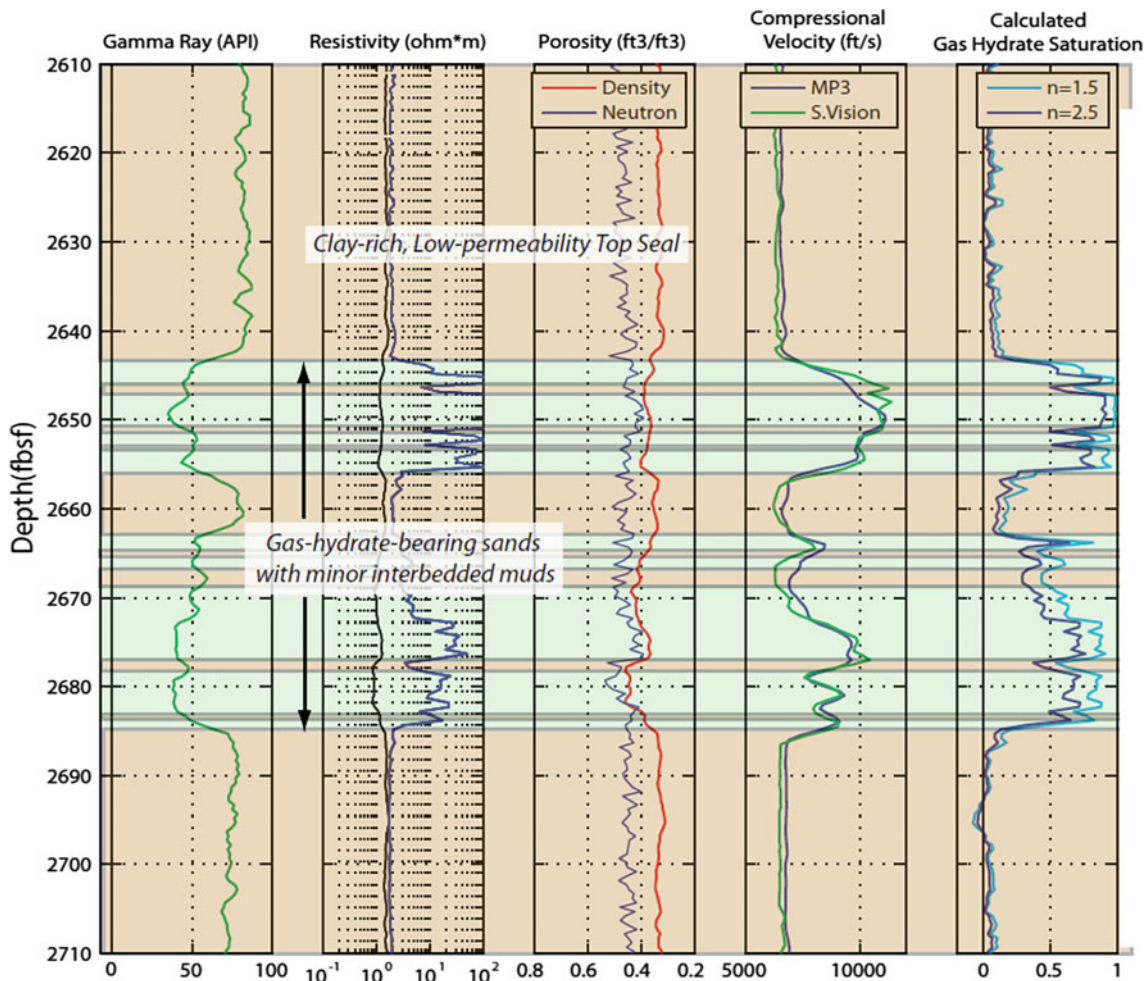


**Fig. 3.13** Downhole logging profiles (from Boswell et al. 2012) from gas hydrate drilling in the Gulf of Mexico (2009) show clear increases in resistivity and P-wave velocity in gas hydrate bearing sands

2016). NASA has therefore focused its astrobiology studies on these crater regions to determine whether microbial life existed in the former oceans of Mars. Regardless, the presence of carbonates implies that at least methane was present on Mars some time in its history, and trace amounts are still observed today (Formisano et al. 2004).

Although Mars has become drier as the ocean slowly vanished around  $\sim 3$  Ga (e.g., Carr and Head 2003; Scheller et al. 2021), some water has still remained in the form of polar ice (Bibring et al. 2004) (Fig. 3.15a) and the ephemeral Recurrent Slope Lineae (RSL), which potentially originated from the seasonal melting of brines on the crater walls (e.g., McEwen et al. 2011). Indeed, the water participating in the hydrological cycle of ancient Mars was lost in space through photo dissociation, stored as subsurface permafrost and in polar caps, and sequestered by crustal hydration (e.g., Scheller et al. 2021).

The ice masses of the polar caps are largely made of frozen water and  $\text{CO}_2$ , which sublimate and freeze between

the summer and winter seasons of Mars (Hvidberg et al. 2012). Winter temperatures near the poles can drop to  $-125$  °C, then increase over the summer months (<https://mars.nasa.gov/all-about-mars/facts/>). The radar image in Fig. 3.15b shows a cross-section of the north polar ice cap on Mars (NASA Mars Reconnaissance Orbiter's Shallow Radar (SHARAD)), featuring layers that indicate an internal ice structure, similar to the ice caps of Earth (e.g., Milkovich and Plaut 2020; Christian et al. 2013). This reflects the climate variability on Mars (e.g., Hvidberg et al. 2012; Becerra et al. 2016; Becerra et al. 2017).

Understanding seasonal changes in gas composition and concentrations in the atmosphere on planetary objects directly above land surface features such as craters (Fig. 3.16) or polar ice caps (Fig. 3.15) may help in deciphering the cause of seasonal swings. For example, the  $\text{CO}_2$  concentrations of Mars decrease when  $\text{CO}_2$  gas freezes over the poles or in craters in the winter, then increase when the  $\text{CO}_2$  evaporates in the spring and summer (Fig. 3.16).

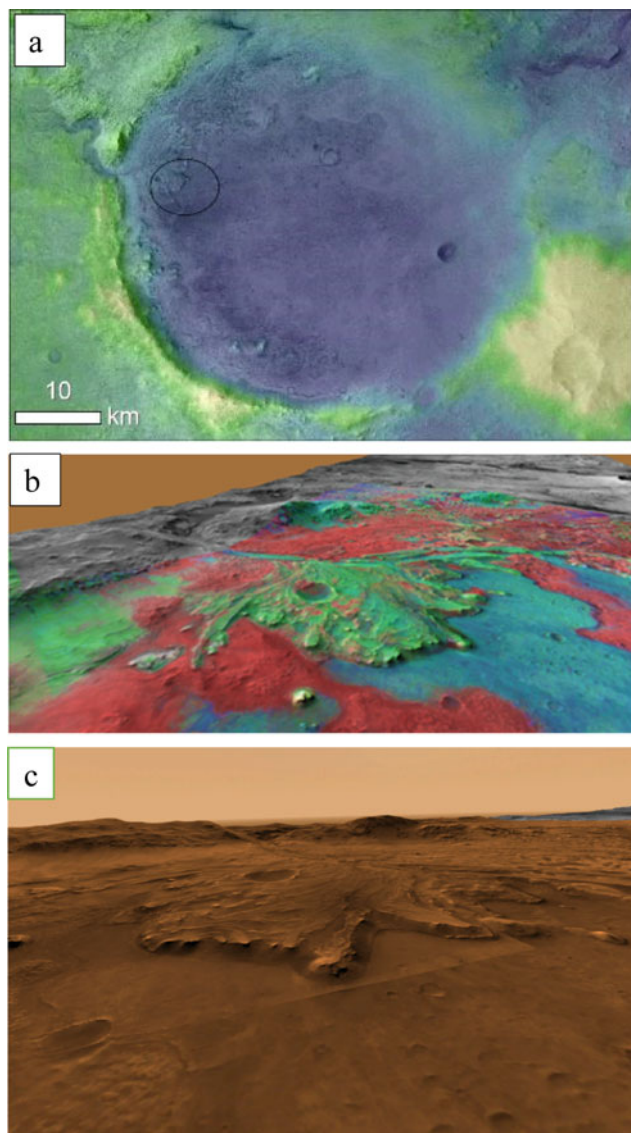


**Fig. 3.14** **a** Image of the Jezero Crater on Mars (landing site 2021 for NASA's Mars 2020 mission), showing channelized depressions indicating former outflows through gaps in the rim of the crater (credit: NASA/JPL-Caltech/MSSS/JHU-APL/ESA). Authigenic carbonates were discovered at the landing site (black circle). **b** Detailed image of the landing site, showing a delta-like outflow region connected to a channelized depression with false colors to highlight morphology and **c** correct colours. A round impact crater also exist elsewhere is visible in the delta

The existence of water and gas are obviously relevant for the existence of hydrates on Mars, in addition to the low temperature and abundance of  $\text{CO}_2$ , which is the dominant gas both in the atmosphere and in the polar ice caps. Even in the shallow subsurface,  $\text{CO}_2$ -dominated clathrates (including methane and noble gases) could be stable over some portions of the Martian seasonal cycle (see e.g., Chastain and Chevrier 2007; Mousis et al. 2013). Measurements reveal, for example,  $\text{CH}_4$  and water vapor maxima above the north

polar cap of Mars during springtime sublimation (Geminale et al. 2011).

Clathrate stability zone conditions are certainly met within the Martian subsurface cryosphere (Clifford et al. 2010; Mousis et al. 2013). The formation of seeps, pockmarks and mud volcanoes are potential indicators of methane hydrate dissociation on Earth, and similar phenomena are also possible on Mars (e.g., Skinner and Mazzini 2009; Komatsu et al. 2011; Oehler and Allen 2010). Although no activity has yet been observed, a fractal analysis of the fracture system underlying the thumb-print terrains of the Arcadia Planitia have shown a source region at the base of the Amazonian gas hydrated cryosphere (De Toffoli et al. 2019).

Methane is occasionally released into the atmosphere of Mars (e.g., Formisano et al. 2004; Mumma et al. 2009; Geminale et al. 2011; Webster et al. 2015; Giuranna et al. 2019). Although one of the most likely sources of methane on Mars is hydrate destabilization, researchers cannot currently determine whether its origin is biological or geological (e.g., magmatic exhalations and serpentinization) (Onstott et al. 2006; Etiope et al. 2011; Etiope and Oehler 2019). More sophisticated analytical methods are needed to definitively determine the source and origin of methane and/or oxygen. Laser spectroscopy methods developed for the oceans of Earth (Jansson et al. 2019) could be a possibility in quantify methane sources on Mars, in its ice caps and on other planetary bodies.

Other clathrate-forming bodies featuring low temperatures ( $< -100$  °C) may also exist elsewhere in the Solar System, including the icy moons of Jupiter and Saturn (Sohl et al. 2010). Indeed, clathrates in the larger moons of Europa, Ganymede, Callisto, Titan, Triton and Enceladus are stable within the lower icy crust and the subsurface ocean. These clathrates may segregate in the ocean based on  $\text{CH}_4$  content; high levels of  $\text{CH}_4$  would cause them to float up to the icy crust/liquid ocean boundary, while low  $\text{CH}_4$  content could cause them to sink, forming a layer at the bottom of the ocean (Sohl et al. 2010; Bouquet et al. 2015). Furthermore, a clathrate layer that caps and insulates a subsurface ocean may act as a thermal insulator, helping to preserve subsurface liquid water and brines on both icy satellites (e.g., Kalousava and Sotin 2020) and larger-sized Kuiper belt objects such as Pluto (Kamata et al. 2019). Enceladus, one of Saturn's moons, even shows evidence of methane plume activity (Fig. 3.17) emanating at the south pole (Porco et al. 2006), which is most likely generated by clathrate decomposition triggered by hydrothermal activity (Kieffer et al. 2006; Bouquet et al. 2015). Whether the methane trapped within clathrates on icy bodies is derived from biogenic or abiogenic chemical processes remains unclear, and this is one of the main motivations for past (e.g., NASA-Dawn; ESA-Cassini), planned (e.g., NASA-Europa-Clipper; ESA-

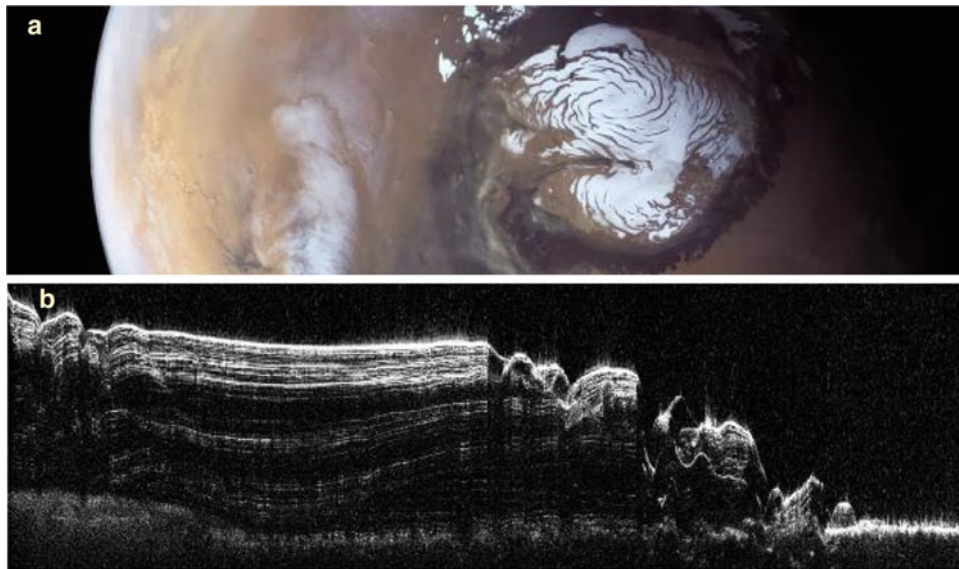


**Fig. 3.15** **a** The northern polar ice cap of Mars is  $\sim 1000$  km (621 miles) across. There are deep troughs within the ice cap that appear as dark, spiral-shaped bands. A  $\sim 2$  km deep canyon almost separates the ice cap. (credit: ESA/DLR/FU Berlin/J. Cowart, CC BY-SA 3.0 IGO). **b** Radar profile shows the internal ice structure of the northern polar ice

cap, with different layers at a southern profile. The profile is  $\sim 2$  km ( $\sim 1.2$  miles) thick and  $\sim 250$  km ( $\sim 155$  miles) across. The individual layers help to reconstruct the paleo surfaces of the ice sheet (credit: NASA/JPL-Caltech/ASI/UT)

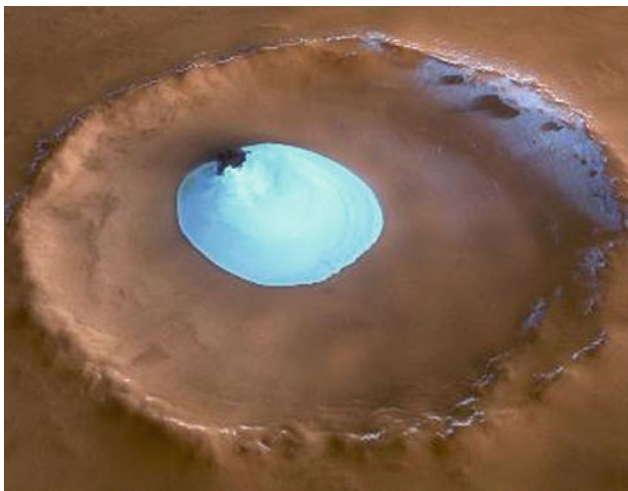


**Fig. 3.16** CO<sub>2</sub> trapped in solid form in a crater on Mars (credit: NASA)

JUICE) and proposed (e.g., NASA-Dragonfly) missions to the icy bodies of the outer Solar System.

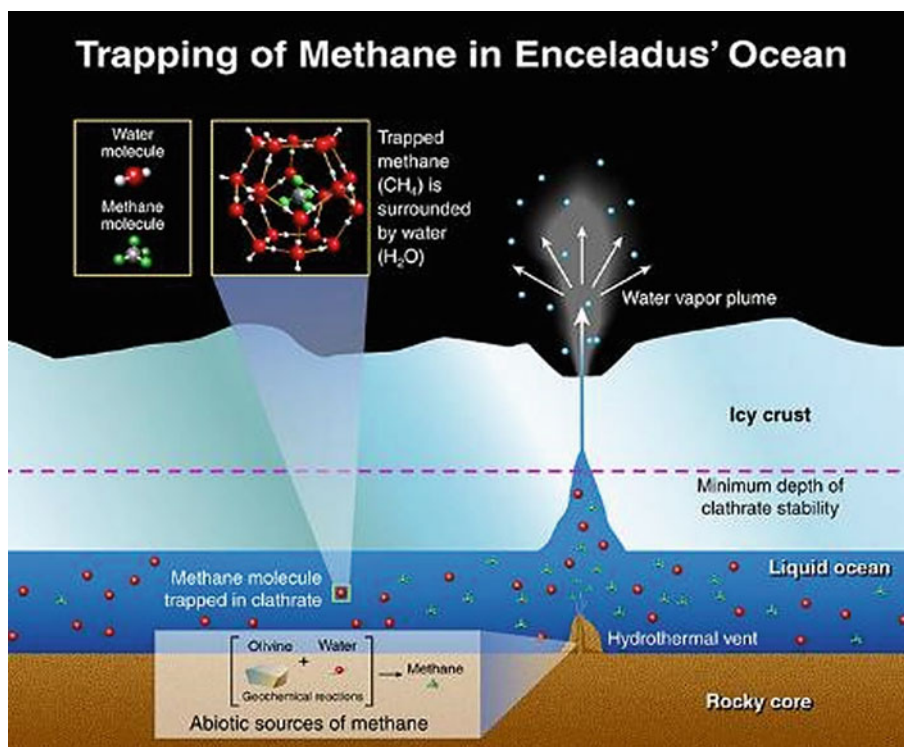
Clathrates have been even detected on the comas of long-period comets (e.g., Bockelée-Morvan et al. 2004; Luspay-Kuti et al. 2015) sourced from the Oort cloud, which are indeed derived from the primordial trapping of the amorphous ice created in the protosolar nebula at temperatures under  $80\text{--}90^\circ\text{K}$  (Schmitt et al. 1989; Rubin et al. 2015; Davidsson et al. 2016). The gas is eventually released through solar heating as the comet approaches the sun.

Exploration on Earth suggests that large amounts of methane are trapped within gas hydrates in sediment along continental margins and in permafrost, while exploration on Mars and other icy satellites suggests the existence of both CO<sub>2</sub> clathrates and CH<sub>4</sub> clathrates under low temperatures. Spectroscopic studies of gas and ice giants may suggest the existence of hydrates on these bodies as well. The effects of seasonal and long-term temperature variations on methane seepage activity remain an important area for research in the Earth's ocean and permafrost regions, particularly for assessing climate-hydrate interactions and microbial feedback mechanisms. Research in the Arctic has demonstrated that cold seeps trap and store more methane in the cold seasons, which is then released in the summer months (Ferré et al. 2020). Such seasonal 'clathrate guns' may exist on Mars, the moons of Jupiter and other icy bodies. Our understanding of Earth's carbon storage and release system may guide future generations of space explorers in searching for microbial life, clathrates and water resources elsewhere in the Solar System and beyond.

### 3.6 Summary

The gas hydrates of Earth are found in the uppermost several hundred meters below the seafloor in continental margins and below Arctic permafrost regions, in areas where enough organic matter exists for biogenic gas production to saturate the pore water with methane. This results in enough free gas

**Fig. 3.17** The ocean of Enceladus, one of the 75 moons of Saturn, may possibly release methane in major plumes. This methane may stem from biogenic or abiogenic chemical processes. The existence and dissociation of methane clathrates provides a physical mechanism and viable hypothesis for the origin of these plumes (credit: NASA, Southwest Research Institute, The Cassini-Huygens mission is a cooperative project of NASA, the European Space Agency and the Italian Space Agency)



for hydrates to form in the subsurface, where temperatures are cold and the pressure is high. Apart from these necessary conditions, the stability of gas hydrates also depends on gas and pore water composition, with higher-order gases increasing the hydrate stability field. While gas hydrate reservoirs on Earth contain mainly methane, the exploration of Mars and other icy satellites such as Jupiter and Saturn suggest the existence of both  $\text{CO}_2$  clathrates and  $\text{CH}_4$  clathrates at low temperatures. Natural gas hydrates contain one of the largest known carbon reservoirs on Earth, and possibly in outer space.

To identify the distribution areas of gas hydrates on Earth, geophysical surveys and drilling operations were conducted along continental margins and in permafrost regions. This led to the conclusion that gas hydrates are widespread on both active and passive margins.

Our ability to utilize natural gas hydrate systems as potential energy resources and/or carbon sinks within the next decade depends on our success in evaluating the environmental risks associated with global clean energy developments and the sequestration of  $\text{CO}_2$ .

The assessment of global warming and other environmental change scenarios associated with the Industrial Age and its impact on methane hydrates remains a critical component in methane hydrate research. Key focus areas include: (a) the assessment of the future stability of gas hydrates within the sedimentary environments that host hydrates, (b) identifying the amount of methane released

from gas hydrates into the ocean and atmosphere, and (c) the impact of methane hydrate dissociation on ocean life.

Greater knowledge and insights into ice sheet melting and methane resource responses are needed, including the quantification of fresh water trapped in the hydrates of Earth and other planetary bodies. This increasing knowledge of water resources on other planets, gas hydrates on Earth, and clathrates and microbial life in outer space may help to constrain the history of the oceans in our planetary system.

## References

- Andreassen K, Berteussen K, Sognnes H et al (2003) Multicomponent ocean bottom cable data in gas hydrate investigation offshore of Norway. *J Geophys Res* 108(B8):2399. <https://doi.org/10.1029/2002JB002245>
- Archer D, Buffett B (2005) Time-dependent response of the global ocean clathrate reservoir to climatic and anthropogenic forcing. *Geochem Geophys* 6(3). <https://doi.org/10.1029/2004GC000854>
- Archer D, Buffett B, Brovkin V (2009) Ocean methane hydrates as a slow tipping point in the global carbon cycle. *Proc Natl Acad Sci* 106(49):20596–20601. <https://doi.org/10.1073/pnas.0800885105>
- Beaudoin YC, Dallimore SR, Boswell R (eds) (2014a) Frozen heat: a UNEP global outlook on methane gas hydrates. Vol 2. United Nations Environment Programme, GRID-Arendal
- Beaudoin YC, Waite WF, Boswell R et al (2014b) Frozen heat, vol 1, pp 1–80. United Nations Environment Programme, GRID-Arendal
- Becerra P, Byrne S, Sori MM et al (2016) Stratigraphy of the north polar layered deposits of Mars from High Resolution Topography. *J Geophys Res* 121:1445–1471. <https://doi.org/10.1002/2015JE004992>



- Becerra P, Sori MM, Byrne S (2017) Signals of astronomical climate forcing in the exposure topography of the North Polar Layered Deposits of Mars. *Geophys Res Lett* 44(1):62–70. <https://doi.org/10.1002/2016GL071197>
- Bibring JP, Langevin Y, Poulet F et al (2004) Perennial water ice identified in the south polar cap of Mars. *Nature* 428:627–630. <https://doi.org/10.1038/nature02461>
- Bockelée-Morvan D, Biver N, Colom P et al (2004) The outgassing and composition of Comet 19P/Borrelly from radio observations. *Icarus* 167(1):113–128. <https://doi.org/10.1016/j.icarus.2003.04.001>
- Boetius A, Ravensschlag K, Schubert CJ et al (2000) A marine microbial consortium apparently mediating anaerobic oxidation of methane. *Nature* 407:623–626
- Boetius A, Wenzhöfer F (2013) Seafloor oxygen consumption fuelled by methane from cold seeps. *Nat Publ Group* 1–10. <https://doi.org/10.1038/ngeo1926>
- Borowski WS, Paull CK, Ussler W (1999) Global and local variations of interstitial sulfate gradients in deep-water, continental margin sediments: sensitivity to underlying methane and gas hydrates. *Mar Geol* 159:131–154. [https://doi.org/10.1016/S0025-3227\(99\)00004-3](https://doi.org/10.1016/S0025-3227(99)00004-3)
- Boswell R, Collett TS (2011) Current perspectives on gas hydrate resources. *Energy Environ Sci* 4(4):1206–1215. <https://doi.org/10.1039/C0EE00203H>
- Boswell R, Collett TS, Frye M et al (2012) Subsurface gas hydrates in the northern Gulf of Mexico. *Mar Pet Geol* 34(1):4–30. <https://doi.org/10.1016/j.marpetgeo.2011.10.003>
- Boswell R, Hancock S, Yamamoto K et al (2020) 6—natural gas hydrates: status of potential as an energy resource. In: Letcher TM (ed) *Future energy*, 3rd edn. Elsevier, pp 111–131
- Bouquet A, Mousis O, Waite JH et al (2015) Possible evidence for a methane source in Enceladus' ocean. *Geophys Res Lett* 42(5):1334–1339. <https://doi.org/10.1002/2014GL063013>
- Bryn P, Berg K, Stoker MS et al (2005) Contourites and their relevance for mass wasting along the Mid-Norwegian Margin. *Mar Pet Geol* 22(1–2):85–96. <https://doi.org/10.1016/j.marpetgeo.2004.10.012>
- Bünz S, Mienert J (2004) Acoustic imaging of gas hydrate and free gas at the Storegga Slide. *J Geophys Res* 109(B4):4102–4115. <https://doi.org/10.1029/2003JB002863>
- Bünz S, Mienert J, Vanneste M et al (2005) Gas hydrates at the Storegga Slide: constraints from an analysis of multicomponent, wide-angle seismic data. *Geophysics* 70(5):B19–B34. <https://doi.org/10.1190/1.2073887>
- Carr MH, Head JW (2003) Oceans on Mars: an assessment of the observational evidence and possible fate. *J Geophys Res E: Planets* 108(5). <https://doi.org/10.1029/2002je001963>
- Chand S, Minshull TA (2003) Seismic constraints on the effects of gas hydrate on sediment physical properties and fluid flow: a review. *Geofluids* 3:275–289
- Chastain BK, Chevrier V (2007) Methane clathrate hydrates as a potential source for martian atmospheric methane. *Planet Space Sci* 55:1246–1256
- Christian S, Holt JW, Byrne S et al (2013) Integrating radar stratigraphy with high resolution visible stratigraphy of the north polar layered deposits. *Mars Icarus* 226(2):1241–1251. <https://doi.org/10.1016/j.icarus.2013.07.003>
- Clifford SM, Lasue J, Heggy E et al (2010) Depth of the Martian cryosphere: revised estimates and implications for the existence and detection of subpermafrost groundwater. *J Geophys Res* 115(E7):1–17. <https://doi.org/10.1029/2009je003462>
- Clifford SM, Parker TJ (2001) The evolution of the Martian hydrosphere: implications for the fate of a primordial ocean and the current state of the Northern plains. *Icarus* 154(1):40–79. <https://doi.org/10.1006/icar.2001.6671>
- Collett TS (1993) Natural Gas Production from Arctic Gas Hydrates. In: Howell DG, Wiese K, Fanelli M et al (eds) *The future of energy gases*. United States Geological Survey, Washington, pp 299–311
- Collett TS (1999) Detailed evaluation of gas hydrate reservoir properties using JAPEX/JNOC/GSC Mallik 2L-38 gas hydrate research well downhole well-log displays (1999) *Bull Geol Surv Canada* (544):295–311
- Collett TS, Boswell R, Lee MW et al (2012) Evaluation of long-term gas hydrate-production testing locations on the Alaska North Slope. *SPE Reserv Eval Eng* 15(2):243–264
- Collett TS, Johnson AH, Knapp CC and Boswell R (2009) Natural gas hydrates: a review. In: Collett T, Johnson A, Knapp C et al (eds) *Natural gas hydrates—Energy resource potential and associated geologic hazards*. AAPG Memoir 89:146–219
- Collett TS, Lee MW, Agena W et al (2011) Permafrost-associated natural gas hydrate occurrences on the Alaska North Slope. *Mar Pet Geol* 28(2):279–294
- Crutchley GJ, Klaeschen L, Bialas J et al (2014) The impact of fluid advection on gas hydrate stability: investigations at sites of methane seepage offshore Costa Rica. *Earth Planet Sci Lett* 401:95–109. <https://doi.org/10.1016/j.epsl.2014.05.045>
- Dallimore SR, Uchida T, Collett TS (eds) (1999) Scientific results from the JAPEX/JNOC/GSC Mallik 2L-38 gas hydrate research well, Mackenzie Delta, Northwest Territories, Canada. *Geol Sur Canada Bull* 544
- Dallimore SR, Wright JF, Nixon FM et al (2008) Geologic and porous media factors affecting the 2007 production response characteristics of the JOGMEC/NRCAN/AURORA mallik gas hydrate production research well. In: *Proceedings, 6th international conference on gas hydrates, 6–10 July 2008, Vancouver, British Columbia, Canada*
- Davidsson BJR, Sierks H, Guttler C et al (2016) The primordial nucleus of comet 67P/Churyumov-Gerasimenko. *Astron Astrophys* 63. <https://doi.org/10.1051/0004-6361/201526968>
- De Batist M, Klerkx J, Van Rensbergen P et al (2002) Active hydrate destabilisation in Lake Baikal, Siberia? *Terra Nova* 14(6):436–442
- Decourt B, Alias S, Debarre R et al (2015) Taking the heat out of the burning-ice debate: Potential and future of Gas Hydrates. In: *SPE Asia Pacific unconventional resources conference and exhibition. Society of Petroleum Engineers*
- Delescluse M, Nedimović MR, Loudon KE (2011) 2D waveform tomography applied to long-streamer MCS data from the Scotian Slope. *Geophysics* 76(4):B151–B163. <https://doi.org/10.1190/1.3587219>
- Dessandier PA, Borrelli C, Yao H et al (2020) Foraminiferal  $\delta^{18}\text{O}$  reveals gas hydrate dissociation in Arctic and North Atlantic ocean sediments. *Geo-Mar Lett* 40:507–523. <https://doi.org/10.1007/s00367-019-00635-6>
- De Toffoli B, Pozzobon R, Massironi M et al (2019) Surface expressions of subsurface sediment mobilization rooted into a gas hydrate-rich cryosphere on Mars. *Sci Rep* 9(1):1–9. <https://doi.org/10.1038/s41598-019-45057-7>
- Dickens GR (2011) Down the Rabbit Hole: toward appropriate discussion of methane release from gas hydrate systems during the Paleocene-Eocene thermal maximum and other past hyperthermal events. *Clim past* 7(3):831–846. <https://doi.org/10.5194/cp-7-831-2011>
- Dickens GR, Castillo MM, Walker JCG (1997) A blast of gas in the latest Paleocene: simulating first-order effects of massive dissociation of oceanic methane hydrate. *Geology* 25(3):259–262. [https://doi.org/10.1130/0091-7613\(1997\)0252.3.CO;2](https://doi.org/10.1130/0091-7613(1997)0252.3.CO;2)
- Egeberg PK, Dickens GR (1999) Thermodynamic and pore water halogen constraints on gas hydrate distribution at ODP Site 997, Blake Ridge. *Chem Geol* 153:53–79

- Ehlert D, Zickfeld K (2017) What determines the warming commitment after cessation of CO<sub>2</sub> emissions? *Environ Res Lett* 12(1). <https://doi.org/10.1088/1748-9326/aa564a>
- Etiopio G, Oehler DZ (2019) Methane spikes, background seasonality and non-detections on Mars: ageological perspective. *Planet Space Sci* 168:52–61. <https://doi.org/10.1016/j.pss.2019.02.001>
- Etiopio G, Oehler DZ, Allen CC (2011) Methane emissions from earths degassing: implications for Mars. *Planet Space Sci* 59(2–3):182–195. <https://doi.org/10.1016/j.pss.2010.06.003>
- Ferré B, Jansson PG, Moser M et al (2020) Reduced methane seepage from Arctic sediments during cold bottom-water conditions. *Nat Geosci* 13(2):144–148. <https://doi.org/10.1038/s41561-019-0515-3>
- Formisano V, Atreya S, Encrenaz T et al (2004) Detection of methane in the atmosphere of Mars. *Science* 306(5702):1758–1761. <https://doi.org/10.1126/science.1101732>
- Geminale A, Formisano V, Sindoni G (2011) Mapping methane in Martian atmosphere with PFS-MEx data. *Planet Space Sci* 59:137–148
- Ginsburg GD, Soloviev VA (1998) Submarine gas hydrates. ISBN 5–8894–013–9 copyright © 1994. Translated from the Russian book edited by V.L. Ivanov VNIIOkeangeologia, St.Petersburg 1994
- Giuranna M, Viscardi S, Daerden F et al (2019) Independent confirmation of a methane spike on Mars and a source region east of Gale Crater. *Nat Geosci* 12(5):326–332. <https://doi.org/10.1038/s41561-019-0331-9>
- Goldberg DS, Collett TS, Hyndman RD (2000) Ground truth: In-situ properties of hydrate. In: Max MD (ed) *Natural gas hydrate*. pp 295–310
- Goldberg DS, Kleinberg RL, Weinberger JL et al (2010) Evaluation of natural gas-hydrate systems using borehole logs. In: Riedel M, Willoughby EC, Chopra S (eds) *Geophysical characterization of gas hydrates*. pp 239–261
- Goldberg DS, Saito S (1998) Detection of gas hydrates using downhole logs. In: Henriot J-P, Mienert J (eds) *Gas hydrates: relevance to world margin stability and climate change*. London: Geological Society of London, vol 137, pp 129–132. <https://doi.org/10.1144/GSL.SP.1998.137.01.09>
- Hafliadon H, Lien R, Sejrup HP et al (2005) The dating and morphometry of the Storegga Slide. *Mar Pet Geol* 22(1–2):123–136. <https://doi.org/10.1016/j.marpetgeo.2004.10.008>
- Helgerud MB, Dvorkin J, Nur A (2000) Rock physics characterization for gas hydrate reservoirs - elastic properties. *Ann NY Acad Sci* 912:116–125
- Helgerud MB, Dvorkin J, Nur A et al (1999) Elastic-wave velocity in marine sediments with gas hydrates: effective medium modeling. *Geophys Res Lett* 26:2021–2024
- Henriet JP, Mienert J (1998) Gas Hydrates: Relevance for World margin stability and climate change. *Geol Soc London Spec Pub* 137. <https://doi.org/10.1144/GSL.SP.1998.137.01.27>
- Higgins JA, Schrag DP (2006) Beyond methane: Towards a theory for the Paleocene-Eocene thermal maximum. *Earth Planet Sci Lett* 245(3–4):523–537. <https://doi.org/10.1016/j.epsl.2006.03.009>
- Holland M, Schultheiss P, Roberts J et al (2008) Observed gas hydrate morphologies in marine sediments. In: Presented at the the international conference on gas hydrates ICGH, Vancouver, British Columbia, CA, pp 1–7
- Horgan BHN, Anderson RB, Dromart G et al (2020) The mineral diversity of Jezero crater: Evidence for possible lacustrine carbonates on Mars. *Icarus* 339. <https://doi.org/10.1016/j.icarus.2019.113526>
- Hvidberg CS, Fishbaugh KE, Winstrup M et al (2012) Reading the climate record of the Martian polar layered deposits. *Icarus* 221(1):405–419. <https://doi.org/10.1016/j.icarus.2012.08.009>
- Jadhawar P, Yang J, Chapoy A, Tohidi B (2021) Sequestration and storage in methane hydrate reservoirs combined with clean methane energy recovery. *Energy Fuels* 35(2):1567–1579. <https://doi.org/10.1021/acs.energyfuels.0c02839>
- Jansson P, Triest J, Grilli R et al (2019) High-resolution underwater laser spectrometer sensing provides new insights into methane distribution at an Arctic seepage site. *Ocean Sci* 15(4):1055–1069. <https://doi.org/10.5194/os-15-1055-2019>
- Johnson AH (2011) Global resource potential of gas hydrate—a new calculation. *Fire in the Ice* 11(2):1–4
- Kalousová K, Sotin C (2020) The insulating effect of methane clathrate crust on Titan’s thermal evolution. *Geophys Res Lett* 47(13):1–9. <https://doi.org/10.1029/2020GL087481>
- Kamata S, Nimmo F, Sekine Y et al (2019) Pluto’s ocean is capped and insulated by gas hydrates. *Nat Geosc* 12:407–410. <https://doi.org/10.1038/s41561-019-0369-8>
- Kastner M, Kvenvolden KA, Whiticar MJ et al (1995) Relationship between pore fluid chemistry and gas hydrates associated with bottom-simulating reflectors at the Cascadia Margin, Sites 889 and 892. In: Carson B, Westbrook GK, Musgrave RJ et al (eds) *Proceedings of the Ocean Drilling Program, Scientific Results 146(Pt 1)*, pp175–187
- Kayen RE, Lee HJ (1991) Pleistocene slope instability of gas hydrate-laden sediment on the Beaufort Sea Margin. *Mar Geotechnol* 10:125–141
- Kennett JP, Cannariato KG, Hendy IL et al (2000) Carbon isotopic evidence for methane hydrate instability during Quaternary interstadials. *Science* 288(5463):128–133. <https://doi.org/10.1126/science.288.5463.128>
- Kennett JP, Cannariato KG, Hendy IL et al (2003) Methane hydrates in Quaternary climate change: the clathrate gun hypothesis. *Am Geophys Union* 216. <https://doi.org/10.1029/054SP01>
- Kieffer SW, Lu X, Bethke CM et al (2006) A clathrate reservoir hypothesis for enceladus south polar plume. *Science* 314(5806):1764–1766. <https://doi.org/10.1126/science.1133519>
- Knittel K, Boetius A (2009) Anaerobic oxidation of methane: progress with an unknown process. *Ann Rev Microbiol* 63:311–334. <https://doi.org/10.1146/annurev.micro.61.080706.093130>
- Komatsu G, Ori GG, Cardinale M et al (2011) Roles of methane and carbon dioxide in geological processes on Mars. *Planet Space Sci* 59(2–3):169–181. <https://doi.org/10.1016/j.pss.2010.07.002>
- Kretschmer K, Biastoch A, Rüpke L et al (2015) Modeling the fate of methane hydrates under global warming. *Global Biogeochem Cy* 29(5):610–625. <https://doi.org/10.1002/2014GB005011>
- Kvenvolden KA (1993) Gas hydrates as a potential energy source—a review of their methane content. In: Howell DG (ed) *The future of energy gases*. US Geological Survey Professional Paper 1570, pp 555–61
- Kvenvolden KA (1988) Methane hydrates and global climate
- Kvenvolden KA, Claypool GE, Threlkeld . <https://www.sciencedirect.com/science/article/abs/pii/0146638084900913> CN et al (1984) Geochemistry of a naturally occurring massive marine gas hydrate. *Organ Geochem* 6:703–713. [https://doi.org/10.1016/0146-6380\(84\)90091-3](https://doi.org/10.1016/0146-6380(84)90091-3)
- Kvenvolden KA, Kastner M (1990) Gas hydrates of the Peruvian outer continental margin. In: Suess E, von Huene R et al (eds) *Proceedings of the ocean drilling program, Scientific Results*, vol 112, pp 517–526
- Kvenvolden KA, McDonald TJ (1985) Gas Hydrat. [http://deepseadrilling.org/84/volume/dsdp84\\_23.pdf](http://deepseadrilling.org/84/volume/dsdp84_23.pdf) of the Middle America Trench. [http://deepseadrilling.org/84/volume/dsdp84\\_23.pdf](http://deepseadrilling.org/84/volume/dsdp84_23.pdf), Deep Sea Drilling Project Leg 84. <https://doi.org/10.2973/dsdp.proc.84.123.1985>
- Leynaud D, Sultan N, Mienert J (2007) The role of sedimentation rate and permeability in the slope stability of the formerly glaciated Norwegian continental margin: the Storegga slide model. *Landslides* 4(4):297–309. <https://doi.org/10.1007/s10346-007-0086-z>

- Long PE, Holland M, Schultheiss P et al. (2010) Infrared imaging of gas-hydrate-bearing cores: state of the art and future prospects. In: Riedel M, Willoughby EC, Chopra S (eds) Geophysical characterization of gas hydrates. Soc Explor Geophys 217–232. <https://doi.org/10.1190/1.9781560802197.ch14>
- Luspay-Kuti A, Hässig M, Fuselier SA et al (2015) Composition-dependent outgassing of comet 67P/Churyumov-Gerasimenko from ROSINA/DFMS: implications for nucleus heterogeneity. *Astron Astrophys* 583:2–9. <https://doi.org/10.1051/0004-6361/201526205>
- MacDonald IR, Bender LC, Vardaro M et al (2005) Thermal and visual time-series at a seafloor gas hydrate deposit on the Gulf of Mexico slope. *Earth Planet Sci Lett* 233(1):45–59
- Makogen YF, Omelchenko RY (2013) Commercial gas production from Messoyakha deposit in hydrate conditions. *J Nat Gas Sci Eng* 11:1–6. <https://doi.org/10.1016/j.jngse.2012.08.002>
- Maslin M, Owen M, Betts R et al (2010) Gas hydrates: past and future geohazard? *philosophical transactions of the royal society a: mathematical. Phys Engi Sci* 368(1919):2369–2393. <https://doi.org/10.1130/G22522.1>
- Masson-Delmotte V, Zhai P, Pörtner HO et al (2018) Global warming of 1.5 C. In: An IPCC special report. World Meteorological Organization, Geneva (2018)
- Mathews MA, Huene von R (1985) Site 570 Methane hydrate zone. In: von Huene R, Aubouin J, Shipboard Scientific Party (eds) Deep sea drilling project initial reports, vol 84, pp 773–790
- McDermott JM, Seewald JS, German CR et al (2015) Pathways for abiotic organic synthesis at submarine hydrothermal fields. *Proc Natl Acad Sci* 112(25):7668–7672. <https://doi.org/10.1073/pnas.1506295112>
- McEwen AS, Ojha L, Dundas CM et al (2011) Seasonal flows on warm martian slopes. *Science* 333(6043):740–743. <https://doi.org/10.1126/science.1204816>
- Mienert J, Berndt K, Laberg JS (2002) Submarine Landslides on Continental Margins. In: Wefer G, Billet G, Hebbel D (eds) Ocean-margin systems. Springer, Heidelberg, pp 179–193
- Mienert J, Vanneste M, Büinz S et al (2005) Ocean warming and gas hydrate stability on the mid-Norwegian margin at the Storegga Slide. *Mar Pet Geol* 22:233–244
- Milkov AV, Etiope G (2005) Global methane emission through mud volcanoes and its past and present impact on the Earth's climate—a comment. *Int J Earth Sci* 94(3):490–492. <https://doi.org/10.1007/s00531-005-0480-5>
- Milkovich SM, Plaut JJ (2020) Martian South Polar layered deposit stratigraphy and implications for accumulation history. *J Geophys Res* 113(E6)
- Mouis O, Chassefière E, Lasue J et al (2013) Volatile trapping in martian clathrates. *Space Sci Rev* 174(1–4):213–250. <https://doi.org/10.1007/s11214-012-9942-9>
- Mumma MJ, Villanueva GL, Novak RE et al (2009) Strong release of methane. *Science* 323:1041–1045. <https://doi.org/10.1126/science.1165243>
- Oehler DZ, Allen CC (2010) Evidence for pervasive mud volcanism in Acidalia Planitia. *Mars Icarus* 208(2):636–657. <https://doi.org/10.1016/j.icarus.2010.03.031>
- Ohgaki K, Takano K, Sangawa H et al (1996) Methane exploitation by carbon dioxide from gashydrates. *J Chem Eng Japan* 29(3):478–483. <https://doi.org/10.1252/jcej.29.478>
- Onstott TC, McGown D, Kessler J et al (2006) Martian CH<sub>4</sub>: sources, flux, and detection. *Astrobiology* 6:2. <https://doi.org/10.1089/ast.2006.6.377>
- Pandey G, Sangwai JS (2020) High pressure rheological studies of methane hydrate slurries formed from water-hexane, water-heptane, and water-decane multiphase systems. *J Nat Gas Sci Eng* 81:103365
- Parkes RJ, Cragg BA, Bale SJ et al (1994) Deep bacterial Biosphere in Pacific-Ocean Sediments. *Nature* 371(6496):410–413
- Paull CK, Dallimore SR, Caress DW et al (2021) A 100-km wide slump along the upper slope of the Canadian Arctic was likely preconditioned for failure by brackish pore water flushing. *Mar Geol* 435. <https://doi.org/10.1016/j.margeo.2021.106453>
- Paull CK, Matsumoto R, Wallace PJ et al (1996) Proceedings of the ocean drilling program. Initial Rep, vol 164
- Piñero E, Marquardt M, Hensen C et al (2013) Estimation of the global inventory of methane hydrates in marine sediments using transfer functions. *Biogeosciences* 10(2):959–975. <https://doi.org/10.5194/bg-10-959-2013>
- Porco CC, Helfenstein P, Thomas PC et al (2006) Cassini observes the active south pole of Enceladus. *Science* 311:1393–1401. <https://doi.org/10.1126/science.1123013>
- Rehder G, Schneider von Deimling J, cruise participants (2008) RV Sonne Cruise report SO 196, SUMSUN 2008, Suva Guam Okinawa trough Manila, 19 February–26 March. <https://epic.awi.de/id/eprint/29645/>, <https://epic.awi.de/id/eprint/29645/>, Leibniz Institut für Ostseeforschung, Sektion Meereschemie, Warnemünde, Bremerhaven, PANGAEA. hdl:10013/epic.35734
- Riedel M, Willoughby E, Chopra S (eds) (2010) Geophysical characterization of gas hydrates. In: society for exploration geophysics. *Geophys Dev Ser* #14:412
- Rubin M, Altwegg K, Balsiger H (2015) Molecular nitrogen in comet 67P/Churyumov-Gerasimenko indicates a low formation temperature. *Science* 348(6231):232–235. <https://doi.org/10.1126/science.aaa6100>
- Ruppel CD, Herman BM, Brothers LL et al (2016) Subsea ice-bearing permafrost on the U.S. Beaufort Margin: 2. Borehole constraints. *Geochem Geophys* 17(11):4333–4353. <https://doi.org/10.1002/2016GC006582>
- Ruppel CD, Kessler JD (2017) The interaction of climate change and methane hydrates. *Rev Geophys* 55:126–168. <https://doi.org/10.1002/2016RG000534>
- Sahling H, Borowski C, Escobar-Briones E et al (2016) Massive asphalt deposits, oil seepage, and gas venting support abundant chemosynthetic communities at the Campeche Knolls, southern Gulf of Mexico. *Biogeosciences* 13(15):4491–4512. <https://doi.org/10.5194/bg-13-4491-2016>
- Saito S, Goldberg D (1997) Evolution of tectonic compaction in the Barbados accretionary prism: estimates from logging-while-drilling. *Earth Planet Sci Lett* 148:423–432. [https://doi.org/10.1016/S0012-821X\(97\)00056-3](https://doi.org/10.1016/S0012-821X(97)00056-3)
- Scheller EL, Ehlmann BL, Renyu H et al (2021) Log-term drying of Mars by sequestration of ocean-scale volumes of water in the crust. *Science* 7717
- Scherwath M, Thomsen L, Riedel M et al (2019) Ocean observatories as a tool to advance gas hydrate research. *Earth Space Sci* 6:2644–2652. <https://doi.org/10.1029/2019EA000762>
- Schmitt B, Espinasse S, Grim JA et al (1989) Laboratory studies of cometary ice analogues. *Phys Mech Cometary Mater* 302:68–70
- Shipley TH, Houston MH (1979) Seismic evidence for widespread possible gas hydrate horizons on continental slopes and rises. *AAPG Bull* 63. <https://doi.org/10.1306/2F91890A-16CE-11D7-8645000102C1865D>
- Singh SC, Minshull TA, Spence GD (1993) Velocity structure of a gas hydrate reflector. *Science* 260(5105):204–207
- Skinner JA, Mazzini A (2009) Martian mud volcanism: terrestrial analogs and implications for formation scenarios. *Mar Pet Geol* 26(9):1866–1878. <https://doi.org/10.1016/j.marpetgeo.2009.02.006>
- Sloan ED Jr (1998) Gas hydrates: review of physical/chemical properties. *Energ Fuel* 12(2):191–196
- Sloan ED, Koh C (2008) Clathrate hydrates of natural gases, 3rd edn. CRC Press
- Snyder F, Dutta N, Hutchinson D et al. (2004) seismic analysis and characterization of gas hydrates in the Northern Deepwater Gulf of

- Mexico. AAPG Bull 88:13. <https://www.researchgate.net/publication/237747646>
- Sohl F, Choukroun M, Kargel J et al (2010) Subsurface water oceans on icy satellites: chemical composition and exchange processes. Space Sci Rev 153(1–4):485–510. <https://doi.org/10.1007/s11214-010-9646-y>
- Stoll RD, Ewing J, Bryan GM (1971) Anomalous wave velocities in sediments containing gas hydrates. J Geophys Res 76(8):2090–2094. <https://doi.org/10.1029/JB076i008p02090>
- Sultan N, Cochonat P, Foucher JP et al (2004) Effect of gas hydrates melting on seafloor slope instability. Mar Geol 213(1–4):379–401. <https://doi.org/10.1016/j.margeo.2004.10.015>
- Thomsen L, Barnes C, Best M et al (2012) Ocean circulation promotes methane release from gas hydrate outcrops at the NEPTUNE Canada Barkley Canyon node. Geophys Res Lett 39(16):1–6. <https://doi.org/10.1029/2012GL052462>
- Tomaru H, Torres ME, Matsumoto R et al (2006) Effect of massive gas hydrate formation on the water isotopic fractionation of the gas hydrate system at Hydrate Ridge, Cascadia margin, offshore Oregon. Geochem Geophys 7:Q10001. <https://doi.org/10.1029/2005GC001207>
- Torres ME, Tréhu AM, Cespedes N et al (2008) Methane hydrate formation in turbidite sediments of northern Cascadia, IODP Expedition 311. Earth Planet Sci Lett 271:170–180
- Torres ME, Wallmann K, Tréhu AM et al (2004) Gas hydrate growth, methane transport, and chloride enrichment at the southern summit of Hydrate Ridge, Cascadia margin off Oregon. Earth Planet Sci Lett 226(1–2):225–241. <https://doi.org/10.1016/j.epsl.2004.07.029>
- Treude T, Boetius A, Knittel K et al (2003) Anaerobic oxidation of methane above gas hydrates (Hydrate Ridge, OR). Mar Ecol Prog Ser 264:1–14
- Tréhu AM (2006) Gas hydrates in marine sediments: Lessons from scientific ocean drilling. Oceanography 19(4):124–142
- Tréhu AM, Flemings P, Bangs N et al (2004a) Feeding methane vents and gas hydrate deposits at south Hydrate Ridge. Geophys Res Lett 31(23):L23310. <https://doi.org/10.1029/2004GL021286>
- Tréhu AM, Long PE, Torres M et al (2004b) Three-dimensional distribution of gas hydrate beneath southern Hydrate Ridge: constraints from ODP Leg 204. Earth Planet Sci Lett 222(3):845–862
- Tucholke BE, Bryna GM, Ewing JI (1977) Gas-hydrate horizons detected in seismic-profiler data from the western North Atlantic. AAPG Bull 61:698–707
- Ussler W, Paull CK (1995) Effects of ion exclusion and isotopic fractionation on pore water geochemistry during gas hydrate formation and decomposition. Geo-Mar Lett 15:37–44
- Waite WF, Ruppel CD, Boze L-G et al (2020) Preliminary global database of known and inferred gas hydrate locations. US Geol Surv Data Release. <https://doi.org/10.5066/P9IIFVJM>
- Webster CR, Mahaffy PR, Atreya SK et al (2015) Mars methane detection and variability at Gale crater. Science 347(6220):415–417
- Weinberger JL, Brown KM, Long PE (2005) Painting a picture of gas hydrate distribution with thermal images. Geophys Res Lett 32: L04609. <https://doi.org/10.1029/2004GL021437>
- Westbrook GK, Carson B, Musgrave RJ et al (1994) Proc ODP, Init Repts, 146 (Pt 1): College station. TX (ocean Drilling Program). <https://doi.org/10.2973/odp.proc.ir.146-1.1994>
- Westbrook GK, Chand S, Rossi G et al (2008) Estimation of gas hydrate concentration from multi-component seismic data at sites on the continental margins of NW Svalbard and the Storegga region of Norway. Mar Pet Geol 25(8):744–758. <https://doi.org/10.1016/j.marpetgeo.2008.02.003>
- Yamamoto K, Terao Y, Fujii T et al (2014) Operational overview of the first offshore production test of methane hydrates in the Nankai Trough. OTC-25243, pp 11
- You K, Flemings PB, Malinverno A et al (2019) Mechanisms of methane hydrate formation in geological systems. Rev Geophys 57 (4):1146–1196. <https://doi.org/10.1029/2018RG000638>
- Zhu T, Dittrich M (2016) Carbonate precipitation through microbial activities in natural environment, and their potential in biotechnology: a review. Front Bioeng Biotechnol 1–21. [https://doi.org/10.3389/fbioe.2016.00004&domain=pdf&date\\_stamp=2016-01-20](https://doi.org/10.3389/fbioe.2016.00004&domain=pdf&date_stamp=2016-01-20)